The Critical Role of Aqueous-Phase Processes in Aromatic-Derived Nitrogen-Containing Organic Aerosol Formation in Cities with Different Energy Consumption Patterns

Yi-Jia Ma[1,2,3], Yu Xu[2,3]*, Ting Yang[1,2,3], Lin Gui[1,2,3], Hong-Wei Xiao[2,3], Hao Xiao[2,3], and Hua-Yun Xiao[2,3]

[1]School of Environmental Science and Engineering, Shanghai Jiao Tong University, Shanghai 200240, China

[2]School of Agriculture and Biology, Shanghai Jiao Tong University, Shanghai 200240, China

[3]Shanghai Yangtze River Delta Eco-Environmental Change and Management Observation and Research Station, Ministry of Science and Technology, National Forestry and Grassland Administration, Shanghai 200240, China

Yu Xu (E-mail: xuyu360@sjtu.edu.cn)

+8615885507087

Shanghai Jiao Tong University, 800 Dongchuan Road

Abstract. Nitrogen-containing organic compounds (NOCs) impact air quality and human health. Here, the abundance, potential precursors, and main formation mechanisms of NOCs in $PM_{2.5}$ during winter were compared for the first time among Haerbin (coal-dependent for heating), Beijing (natural gas and coal as heating energy), and Hangzhou (no centralized heating policy). The total signal intensity of CHON+, CHN+, and CHON− compounds was highest in Haerbin and lowest in Hangzhou. Anthropogenic aromatics accounted for 73%–93% of all identified precursors of CHON+, CHN+, and CHON− compounds in Haerbin. Although the abundance of aromatics-derived NOCs was lower in Beijing than in Haerbin, aromatics were also the main contributors to NOC formation in Beijing. Hangzhou exhibited the lowest levels of aromatic precursors. Furthermore, non-metric multidimensional scaling analysis indicated an overall reduction in the impact of fossil fuel combustion on NOC pollution along the route from Haerbin to Beijing to Hangzhou. We found that aqueous-phase processes (mainly condensation, hydrolysis or dehydration processes for reduced NOCs, and mainly oxidization or hydrolysis processes for oxidized NOCs) can promote the transformation of precursors to produce NOCs, leading to the most significant increase in aromatic NOC levels in Haerbin (particularly on haze days). Reduced precursor emissions in Beijing and Hangzhou (the lowest) constrained the aqueous-phase formation of NOCs. The overall results suggest that the aerosol NOC pollution in coal-dependent cities is mainly controlled by anthropogenic aromatics

and aqueous-phase processes. Thus, without effective emission controls, the formation of NOCs through aqueous-phase processes may still pose a large threat to air quality.

Keywords: Aerosols, Nitrogen-containing organic compounds, Energy structure, Anthropogenic pollutants, Formation mechanisms

1. Introduction

Nitrogen-containing organic compounds (NOCs) are abundant reactive nitrogen species in aerosol particles, accounting for up to 40%–80% of total nitrogen deposition (Li et al., 2023; Xi et al., 2023; Yu et al., 2020). Clearly, aerosol NOCs can significantly contribute to the global nitrogen cycle (Li et al., 2023; Cape et al., 2011). Moreover, the formation of secondary organic aerosols (SOA) and light-absorbing organic aerosols (e.g., brown carbon) is also tightly associated with NOCs (Wang et al., 2024; Liu et al., 2023b; Zeng et al., 2021), thus affecting the radiative balance and air quality (Yuan et al., 2023; Jiang et al., 2023). In particular, certain NOCs, such as nitroaromatics and peroxyacyl nitrates, are characterized as phytotoxins and potential carcinogens, posing threats to ecosystems and human health (Shi et al., 2023; Singh and Kumar, 2022; Huang et al., 2024). Therefore, understanding the characteristics, origins, and atmospheric processes of NOCs is essential for comprehending their climate and health effects.

Aerosol NOCs can be derived from primary emissions associated with anthropogenic activities and natural sources (Lin et al., 2023; Xu et al., 2020a; Wang et al., 2017; Song et al., 2018; Song et al., 2022; Ma et al., 2024; Gui et al., 2024; Xu et al., 2024a). Secondary formation processes may play a more crucial role in the formation of NOCs in fine aerosol particles, which involve interactions among volatile organic compounds (VOCs), atmospheric oxidants, and reactive inorganic

nitrogen species (Montoya-Aguilera et al., 2018; Perraud et al., 2012; Hallquist et al., 2009). For instance, laboratory studies have observed the formation of organic nitrates from the oxidation of isoprene and α-/β-pinene by atmospheric oxidants and nitrogen oxides (NO_x) (Surratt et al., 2010; Rollins et al., 2012; Nguyen et al., 2015). Additionally, aqueous-phase reactions of NH_4^+ (or NH_3) with biogenic VOCs or carbonyl compounds have been suggested to be important mechanisms of reduced NOC (Re-NOCs) formation (Abudumutailifu et al., 2024; Laskin et al., 2014; Li et al., 2019b; Liu et al., 2023b; Wang et al., 2024). However, understanding the origins, formation mechanisms, and environmental impacts of NOCs is hindered by the elusive and intractable molecular information regarding NOCs and their precursors.

Aerosol liquid water (ALW) can greatly increase the formation of aerosol NOCs by facilitating the conversion of water-soluble organic gases into particles and subsequently enabling aqueous-phase reactions (Li et al., 2019a; Lv et al., 2022; Liu et al., 2023b). Several observational studies have found a positive correlation between aerosol NOC abundance and either ALW or relative humidity (RH) (Jiang et al., 2023; Liu et al., 2023b; Xu et al., 2020b). In particular, it has been suggested that increased ALW levels can exacerbate winter haze in China (Wu et al., 2018; Hodas et al., 2014; Lv et al., 2022; Wang et al., 2021d; Liu et al., 2023b; Wang et al., 2021a; Li et al., 2019a). Presumably, precursors and ALW are the two key factors in the formation of aerosol NOCs. Haze environments have potentially high RH levels and large

emissions of NOC precursors (Zheng et al., 2023; Nie et al., 2022; Liu et al., 2021; Wang et al., 2021a). Moreover, in Chinese cities with different energy consumption (e.g., coal, biomass, and natural gas) for winter heating (Zhang et al., 2021b; Zhang et al., 2023b; Yang et al., 2024c), the types and emission intensities of pollutants released from different heating sources are expected to vary considerably (Bond et al., 2006; Stockwell et al., 2015; Křůmal et al., 2019). However, the potential effects of ALW in the formation of NOCs in Chinese cities with different energy consumption during winter, particularly in haze periods, are not well documented. Moreover, the roles of ALW-related NOC formation processes in the formation of haze in cities with different energy consumption types also remain largely unknown.

In this study, we present the measurements of the NOCs and other chemical compositions in $PM_{2.5}$ collected from three cities (Haerbin, Beijing, and Hangzhou) with different energy consumption during winter. The specific objectives of this study were: (1) to investigate the differences in the abundance, composition, and major precursors of NOCs in different cities with different energy consumption, especially on polluted days; and (2) to elucidate the potential effects of aqueous-phase processes on the formation of oxidized NOCs (Ox-NOCs) and reduced NOCs (Re-NOCs) during winter (particularly on polluted days) in cities with different energy consumption. The research findings are expected to provide valuable implications for the mitigation of aerosol NOCs pollution in urban environments.

2. Materials and methods

2.1. Study site description and sample collection

The study sites are located in three urban areas, including Haerbin (HEB, i.e., Harbin, 126.64°E, 45.77°N), Beijing (BJ, 116.41°E, 40.04°N), and Hangzhou (HZ, 120.16°E, 30.30°N) (**Fig. S1**). The city of HEB, with a population of 9.95 million, is situated in the northeastern region of China. It relies heavily on coal for centralized heating during winter. The rapid urbanization and increased coal consumption have significantly deteriorated air quality in HEB in recent years (Ma et al., 2020). In contrast, BJ has largely shifted towards the utilization of cleaner energy sources (e.g., natural gas) for centralized heating in recent years, particularly following the implementation of the "Beijing 2013–2017 Clean Air Action Plan" (Vu et al., 2019; Yuan et al., 2023). HZ, situated within the Yangtze River Delta, is exempt from the necessity of heating due to the relatively mild winter climate (average temperature of 6.6 ± 2.4 °C during the sampling period, **Table S1**). Clearly, the distinctive energy consumption patterns observed in these three cities during winter provide a valuable opportunity to examine the impact of various precursors and aqueous-phase processes on aerosol NOC formation.

Sample collection was carried out simultaneously in three cities from 16 December 2017 to 14 January 2018. $PM_{2.5}$ samples were collected every two or three

127 days with a duration of 24 hours onto prebaked quartz fiber filters (Pallflex, Pall
128 Corporation, USA) using a high-volume air sampler (Series 2031, Laoying, China).
129 One blank sample was collected at each sampling site. A total of 39 samples were
130 collected, all of which were stored at −30°C. Meteorological data (e.g., temperature,
131 relative humidity (RH) and wind speed) together with concentrations of various
132 pollutants (e.g., SO_2 and NO_2) were obtained from nearby environmental stations. In
133 China, according to the Air Quality Index (MEEPRC, 2012), a pollution day is
134 defined as a day with a 24-hour average $PM_{2.5}$ concentration above 75 μg m^{-3}. This
135 standard has also been used in other studies performed in China (Zhang and Cao,
136 2015; Xu et al., 2024b; Yan et al., 2024), showing that the sampling periods were
137 classified as either "clean" or "haze" based on whether the daily average concentration
138 of $PM_{2.5}$ was below or above 75 μg m^{-3}.
139
140 **2.2. Chemical analysis**
141 The extraction and analysis methods for NOCs were consistent with those
142 described in our recent publication (Ma et al., 2024). Briefly, a portion of each filter
143 was extracted with methanol (LC-MS grade, CNW Technologies Ltd.) using
144 sonication in an ice bath (~4°C). The extracts were filtered through a 0.22 μm
145 polytetrafluoroethylene syringe filter and then concentrated to 300 μL under a gentle
146 stream of nitrogen gas. The concentrated extracts underwent composition analysis via

147 an ultra-performance liquid chromatography coupled with quadrupole time-of-flight
148 mass spectrometry equipped with an electrospray ionization (ESI) source (UPLC-ESI-
149 QToFMS, Waters Acquity Xevo G2-XS) (Wang et al., 2021c; Ma et al., 2024). This
150 analysis was done in both ESI+ and ESI– modes. The organic compounds were
151 separated on an Acquity HSS T3 column (2.1 × 100 mm, 1.8 μm particle size, Waters)
152 with an 18-minute gradient elution. The mobile phases comprised ultrapure water
153 with 0.1% formic acid (A) and methanol with 0.1% formic acid (B). Gradient elution
154 was conducted according to the following protocol: 1% B was held for 1.5 minutes,
155 followed by an increase to 54% B over a period of 6.5 minutes. Thereafter, the B was
156 increased to 95% over a period of 3 minutes. After reaching 100% B in one minute,
157 this state was maintained for 3 minutes. Finally, the concentration was returned to 1%
158 B in 0.5 minutes and held for 2.5 minutes. More detailed information about the
159 UPLC-ESI-QToFMS analysis can be found in **Sect. S1**. Due to uncertainties in
160 ionization efficiencies for different compounds (Ditto et al., 2022; Yang et al., 2023),
161 an intercomparison (mainly compared among samples within this study) of compound
162 relative abundance was conducted without accounting for differences in ionization
163 efficiency in the present study. This consideration was consistent with previous
164 studies (Xu et al., 2023; Jiang et al., 2022; Ma et al., 2024).
165 Another filter portion was ultrasonically extracted using Milli-Q water (~4°C ice
166 bath) to analyze the concentrations of inorganic ions and organic acids. The inorganic

ions (e.g., NO_3^-, SO_4^{2-}, Cl^-, Ca^{2+}, Mg^{2+}, Na^+, and NH_4^+) and organic acids (e.g., formic acid, acetic acid, oxalic acid, succinic acid, glutaric acid, and methanesulfonic acid) were quantified using an ion chromatograph system (Dionex Aquion, Thermo Scientific, USA), as described previously (Xu et al., 2022b; Yang et al., 2024b).

2.3. Compound categorization and precursor identification

The identified molecular formulas via UPLC-ESI-QToFMS were categorized into different compound classes based on their elemental compositions, which included CHO−, CHON−, CHONS−, and CHOS− in ESI− mode and CHO+, CHON+, and CHN+ in ESI+ mode (Ma et al., 2024). Unless otherwise indicated, the molecular formulas presented in the manuscript refer to neutral molecules. The "−" and "+" symbols denote the detection ion modes, which correspond to ESI− and ESI+ modes, respectively. Here, we mainly focus on NOCs (i.e., CHN+, CHON+, and CHON− compounds) (Ma et al., 2024; Jiang et al., 2022; Wang et al., 2017). The carbon oxidation state (OS_C) and double bond equivalent (DBE) were calculated to indicate the oxidation level and unsaturation degree of the organics, respectively (**Sect. S2**) (Kroll et al., 2011; Ma et al., 2024). Additionally, the modified aromaticity index (AI_{mod}) and aromaticity equivalent (X_C) were used to evaluate aromaticity of organics (Koch and Dittmar, 2006), as detailed in **Sect. S2**.

The potential precursors of NOCs were identified based on the methodology

described in previous studies (Nie et al., 2022; Guo et al., 2022; Jiang et al., 2023). The classification of CHON+ and CHON− compounds was refined into the following categories, including aliphatic-, heterocyclic-, and aromatic-derived Re-NOCs and isoprene-, monoterpene-, aliphatic-, and aromatic-derived Ox-NOCs. Moreover, CHN+ compounds were classified into aliphatic, monoaromatic, and polyaromatic CHN+ compounds (Wang et al., 2021b; Yassine et al., 2014). A detailed description of the revised workflow for classifying NOCs according to potential precursors was provided in **Sect. S3** and **Fig. S2**.

2.4. Classification of potential pathways for NOC formation

To identify potential aqueous-phase processes for aerosol NOC formation, we screened precursor-product pairs from the organic compounds that have been detected (Su et al., 2021; Xu et al., 2023; Jiang et al., 2023). The reaction pathways of Re-NOCs (mainly CHON+ compounds in this study) were refined into the following categories, including condensation (cond_N), hydrolysis (hy_N), dehydration (de_N), cond_hy_N (involving cond_N and hy_N), cond_de_N (involving cond_N and de_N), hy_de_N (involving hy_N and de_N), cond_hy_de_N (involving cond_N, hy_N and de_N) and unknown_N (unknown processes) formation pathways (**Fig. S3 and Table S4**) (Sun et al., 2024; Abudumutailifu et al., 2024; Laskin et al., 2014; Liu et al., 2023c). Another significant class of Re-NOCs is the CHN+ compounds. Their

potential formation mechanisms include cond_N, de_N, cond_de_N, and other unidentified (unknown_N) pathways (**Fig. S4** and **Table S4**) (Abudumutailifu et al., 2024; Laskin et al., 2014; Liu et al., 2023c). In addition, the reaction pathways of Ox-NOCs (mainly CHON− compounds in this study) were refined into the following categories, including ox_N, hy_N, ox_hy_N (involving ox_N and hy_N), and other unidentified (unknown_N) pathways (Jiang et al., 2023; Su et al., 2021) (**Fig. S5** and **Table S4**). A detailed overview of the methodologies employed to discern potential NOC formation pathways was shown in **Sect. S4**, **Table S4,** and **Figs. S3–S5**.

It is important to acknowledge the potential limitations in the categorization methodology of NOC formation pathways described above. This is because the approach applied here and in previous studies (Jiang et al., 2023; Su et al., 2021) may classify NOCs as products of aqueous-phase reactions from primary emissions. Accordingly, our results can be regarded as a maximal potential (or an upper limit) for NOC generation from aqueous-phase reactions. In particular, certain reaction pathways (e.g., oligomerization) were not included in this study due to the complexity of the atomic changes involved, which could not be effectively characterized using the "precursor-product pairs" approach. In this study, NOCs produced from the reaction pathways identified by the abovementioned classification methodology can explain 76% of CHON+ compounds, 61% of CHN+ compounds, and 65% of CHON− compounds. Thus, the classification of potential pathways for NOC formation was representative,

at least in this study.

2.5. More parameter calculations and data analysis

A thermodynamic model (ISORROPIA-II) was used to estimate the ALW concentration and pH value, as described in previous studies (Xu et al., 2020b; Xu et al., 2023; Xu et al., 2022c). Ambient hydroxyl radical (•OH) concentrations were predicted using empirical formulas proposed by Ehhalt and Rohrer (2000), which was reported in detail in our previous field observations (Liu et al., 2023a; Lin et al., 2023). The ventilation coefficient (VC) is an indicator of the potential for atmospheric dilution of pollutants, which was calculated by multiplying the wind speed by the planetary boundary layer height (PBLH) (Gani et al., 2019) .

Non-metric multidimensional scaling (NMDS) was employed to visualize the distributions of NOCs (CHON+, CHN+, and CHON– compounds) in two dimensions, based on Bray-Curtis distances (Chao et al., 2006). The stress values ranged from 0.03 to 0.11 (less than 0.2, **Table S5**) in our analysis, indicating that the differences among samples can be well represented in the two-dimensional pattern. To further assess the influence of anthropogenic emissions and aqueous-phase processes on the distribution of NOCs, the envfit function in the R package Vegan (Oksanen et al., 2007) was utilized. Furthermore, the Spearman rank correlation, a non-parametric measure with less sensitivity to outliers and independent of data distribution

assumptions, was employed to examine the association patterns between NOCs and the parameters related to anthropogenic emissions and aqueous-phase processes (Kellerman et al., 2014).

3. Results and discussion

3.1. Overview of pollution and aerosol NOC characteristics in different cities

Figure 1a–c and **Table S1** show the variations in major gaseous pollutants, $PM_{2.5}$ and its major compositions, as well as meteorological parameters in three Chinese cities with different energy consumptions during winter. The average $PM_{2.5}$ concentration in HEB was 90.6 ± 62.4 μg m^{-3}, which was significantly higher than that observed in BJ (52.7 ± 51.4 μg m^{-3}) and HZ (69.1 ± 29.6 μg m^{-3}). Similarly, the concentrations of SO_2 and nss-Cl^- were higher in HEB than in BJ and HZ. In addition, a lower NO_3^-/SO_4^{2-} mass ratio (**Table S1**) was found in HEB. SO_2 and nss-Cl^- have been suggested to be typical pollutants emitted from coal combustion during winter in cities (Zhao and Sun, 1986; Streets and Waldhoff, 2000). The low NO_3^-/SO_4^{2-} mass ratio can indicate a predominance of stationary sources (e.g., coal combustion) (Wang et al., 2006; Arimoto et al., 1996; Xiao and Liu, 2004). These results suggest that coal combustion during the winter heating season in HEB may significantly contribute to severe $PM_{2.5}$ pollution. This consideration can also be supported by the highest coal consumption in HEB in 2017–2018 (**Fig. 1d**). Due to the large-scale use of clean

energy (i.e., natural gas) in BJ (**Fig. 1e**), the coal consumption in BJ was the lowest (**Fig. 1d**). This resulted in the lowest pollutant levels in BJ. From clean to polluted days, HEB and BJ showed larger increases in pollutant levels (e.g., $PM_{2.5}$, SO_2, and CO), followed by HZ. Thus, the release of pollutants caused by the use of fossil fuels for centralized heating in winter (only occurred in HEB and BJ) was undoubtedly one of the important factors contributing to the generation of haze in HEB and BJ.

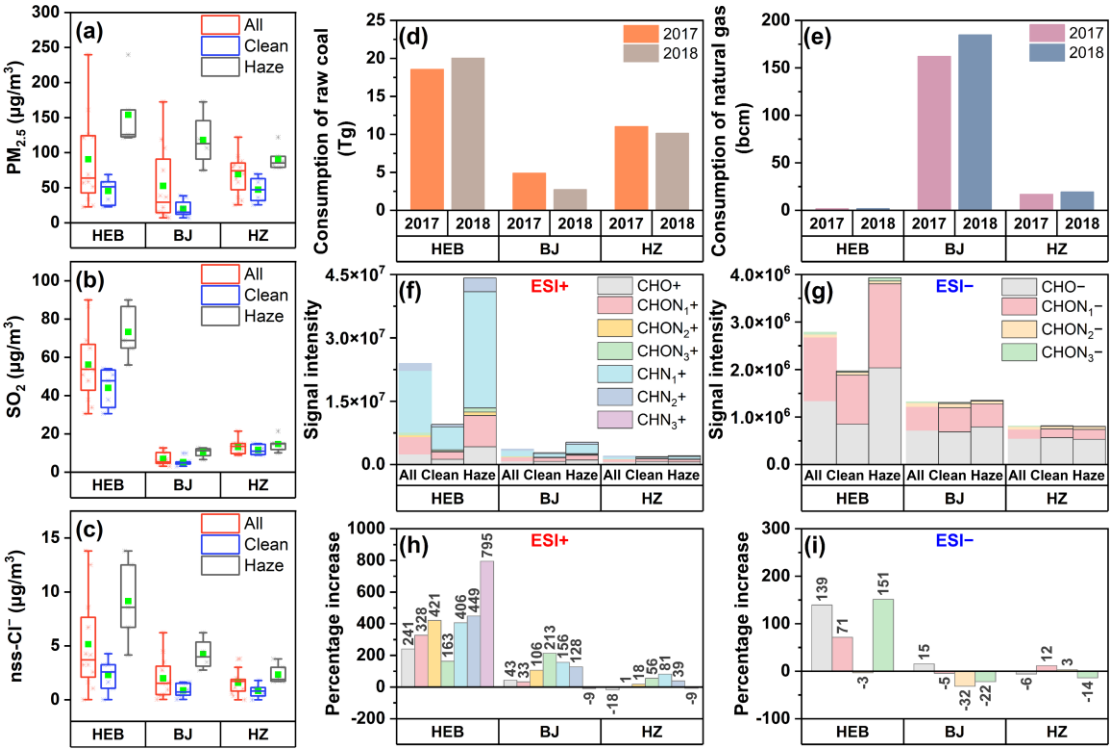

Figure 1. Box and whisker plots showing variations in the concentration of (**a**) $PM_{2.5}$, (**b**) SO_2, and (**c**) nss-Cl^- in all (gray), clean (blue), and haze (red) periods in different cities. Each box encompasses the 25th–75th percentiles. Whiskers are the 5th and 95th percentiles. The green squares and solid lines inside boxes indicate the mean and median values. The consumption of (**d**) raw coal and (**e**) natural gas in 2017 and 2018

in different cities was obtained from the local statistical yearbooks. Average distributions in the signal intensity of species detected in $PM_{2.5}$ collected during different winter periods in different cities in (**f**) ESI+ and (**g**) ESI− modes. Percentage variations in the signal intensity of each subgroup from clean to haze periods in different cities in (**h**) ESI+ and (**i**) ESI− modes.

Figure 1f and **g** show the average signal intensity distributions of organic compounds detected in $PM_{2.5}$ across sampling periods in different cities. The detailed mass spectra of organic compounds detected in ESI+ and ESI− were shown in **Fig. S6**. CHN_1+ (n = 437−448) compounds were the main CHN molecules measured in ESI+ mode in all cities (**Fig. 1f** and **Table S6**), the signal intensity of which accounted for over 77% of the total $CHN_{1–3}$+ signal intensity. Similarly, $CHON_1$+ compounds (n = 398−421) dominated in $CHON_{1–3}$+ molecules, with a higher signal intensity than $CHON_{2–3}$+ (**Fig. 1f** and **Table S6**). The high abundances of CHN_1+ and $CHON_1$+ compounds in NOCs were similar to previous reports about the NOC characteristics of urban aerosols (He et al., 2024; Abudumutailifu et al., 2024). The signal intensity fractions (40%−77%) of CHN+ compounds in total NOCs in these three cities were higher than those observed (8.20%−17.47%) during winter in Ürümqi where the same NOC analysis method was conducted (Ma et al., 2024). However, the signal intensity fractions of CHON+ compounds in total NOCs were lower in these three cities

(23%−60%) than in Ürümqi (over 82.53%) (Ma et al., 2024). More frequent biomass burning and relatively dry climate in Ürümqi (northwest China) (Ma et al., 2024) may result in different sources and formation processes of NOCs compared to this study. The signal intensity of these NOCs detected in ESI+ mode varied across cities, with the highest CHN+ and CHON+ signal intensities in HEB, followed by BJ and HZ. Moreover, we found that the total signal intensities of CHN+ and CHON+ compounds increased by 382% in HEB from clean to haze periods, followed by increase of 102% in BJ and increase of 31% in HZ (**Fig. 1h** and **Table S6**). This variation pattern of CHN+ and CHON+ compounds from clean to haze periods was similar to that of the pollutants mentioned previously (**Fig. 1a**–**c**). Given the high sensitivity of ESI+ mode to protonatable species, reduced species (e.g., amine- and amide-like compounds) were expected to predominate the NOCs (Han et al., 2023; Wang et al., 2018), the formation of which was highly related to precursor emission level, aerosol acidity, and ALW concentrations (Kuwata and Martin, 2012; Vione et al., 2005; Yang et al., 2024a; Xu et al., 2020b). Thus, these results suggest that there may be significant differences in the sources, precursor emission intensity, or main formation pathways of NOCs in different energy consuming cities.

The number of NOCs identified in ESI− (296–301 molecules excluding sulfur-containing compounds, **Table S7**) was found to be lower than that observed in ESI+ (1346–1361) (**Table S6**). This finding was similar to previous observations about the

NOCs of urban organic aerosols in Beijing, Mainz, Changchun, Guangzhou, and Shanghai (Wang et al., 2021b; Wen et al., 2023; Wang et al., 2018). $CHON_1^-$ compounds were the main NOC molecules in ESI− mode in all cities (**Fig. 1g** and **Table S7**). The average signal intensity of CHON− compounds was highest in HEB, followed by BJ and HZ. Moreover, the outbreak of $CHON_{1-3}$ signal intensity during polluted periods was found in HEB, whereas insignificant increases occurred in BJ and HZ (**Fig. 1i**). Deprotonated NOCs with oxidized nitrogen-functional groups, such as nitro ($–NO_2$) or nitrooxy ($–ONO_2$) groups, are more sensitive to the ESI− mode (Wang et al., 2017; Jiang et al., 2023; Yuan et al., 2023). Clearly, the formation of aerosol CHON− compounds was largely dependent on atmospheric oxidation capacity and gas- and aqueous-phase reactions (Ng et al., 2017; Shi et al., 2020; Shi et al., 2023). Thus, the differences in CHON− compound abundance in different polluted periods and cities together with the spatiotemporal changes in CHN+ and CHON+ abundances mentioned previously were likely attributed to variations in sources, mechanisms, or key influencing factors of NOC formation in these three cities, which will be further discussed in the following sections.

3.2. Potential precursors of aerosol NOCs in different cities

Figure 2 presents the average signal intensity percentage and signal intensity distributions of different NOCs from various precursors in different cities during

winter. Aromatics-, heterocyclics-, and aliphatics-derived Re-NOCs together accounted for more than 74% (74%–79%) of the total signal intensity of CHON+ compounds in the three study cities (**Fig. 2a**–**c** and **Table S8**). Specifically, the proportion of the aromatics-derived CHON+ signal intensity in the total CHON+ signal intensity was much higher in HEB (73%) than in BJ (33%), with the lowest proportion observed in HZ (23%) (**Fig. 2a**–**c**). Furthermore, we observed that aromatic CHN+ compounds (mono- and poly-aromatics) dominated the total CHN+ compounds in both number and abundance in all investigated cities (**Table S9** and **Fig. 2d**–**f**). The average signal intensity percentage and signal intensity of aromatic CHN+ compounds were also highest in HEB (**Fig. 2d**–**f** and **k**). The calculated AI_{mod} values for CHON+ and CHN+ compounds were higher in HEB than in BJ and HZ (**Table S10**), which further indicated a higher aromaticity of these NOCs in HEB. It has been suggested that coal combustion can release a large amount of aromatic compounds (Zhang et al., 2023a), which potentially increased NOC aromaticity (Yuan et al., 2023). Thus, the higher signal proportion of aromatics-derived Re-NOCs in HEB can be explained by the higher coal combustion emissions during winter. In contrast, the use of clean energy during the central heating season in BJ and the reduced emissions in HZ without central heating weakened the formation of aerosol aromatic NOCs.

CHON− compounds were also primarily dominated by aromatics-derived Ox-NOCs in all three cities, accounting for more than 73% (73%–90%) of the total signal

intensity of CHON− compounds, on average (**Fig. 2g–i**). This finding was consistent with field observations conducted in other Chinese cities such as Shanghai, Changchun, Guangzhou, and Wangdu during winter (Wang et al., 2021b; Jiang et al., 2023). The abundance of aromatics-derived Ox-CHON− compounds and the AI_{mod} value of CHON− were highest in HEB and decreased sequentially in BJ and HZ (**Fig. 2l** and **Table S10**), further indicating our previous consideration that coal combustion heating in HEB can lead to higher NOC pollution. It is worth noting that the percentage of total signal intensity of Ox-NOCs with biogenic VOCs (BVOCs) as precursors was less than 3% (**Fig. 2g–i** and **Table S8**). This can be partly supported by the previous observations showing that anthropogenic VOCs (AVOCs) were the main contributors to the formation of Ox-NOCs (e.g., organic nitrates) in urban areas in China (Wang et al., 2021b; Jiang et al., 2023). The overall results suggest the significant role of AVOCs in the formation of NOCs in all investigated cites, particularly in HEB.

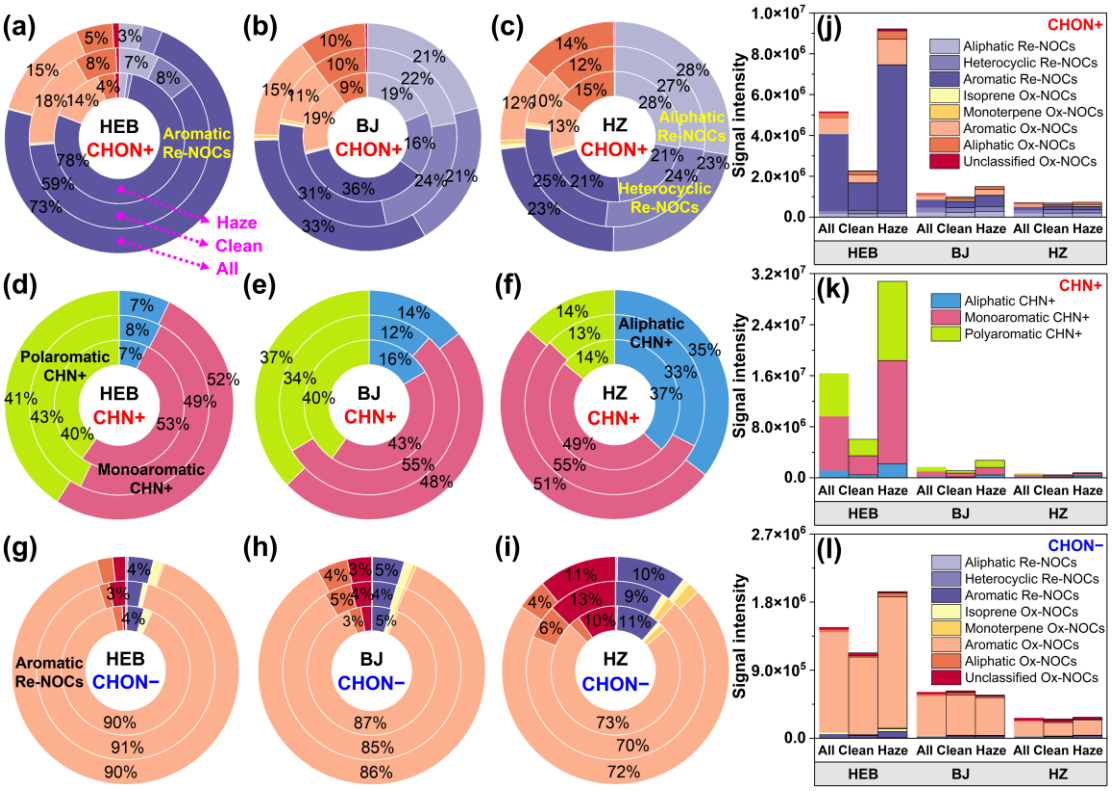

Figure 2. Average percentage distributions of signal intensities for (**a**–**c**) CHON+, (**d**–**f**) CHN+, and (**g**–**i**) CHON− compounds from various sources in $PM_{2.5}$ collected from different cities during winter. Average signal intensity distributions for (**j**) CHON+, (**k**) CHN+, and (**l**) CHON− compounds from various sources in $PM_{2.5}$ collected from different cities during winter.

From clean to haze periods, the signal intensities of all aromatics-derived CHON compounds increased significantly in HEB (**Figs. 2a, j, g, l** and **S7**). In contrast, the signal intensities of aromatics-derived CHON compounds in BJ and HZ showed an insignificant increase during haze periods. In addition, the average values of O/C_w and OS_{Cw} for CHON+ and CHON− compounds were higher in HEB than in BJ (second

highest) and HZ, and their increases from clean to haze periods were also greater in HEB (**Table S10**). Concurrently, the O/C_w ratio of aerosol NOCs in HEB was observed to be higher than that of coal-derived aerosols (Song et al., 2018). Heald et al. (2010) previously demonstrated that oxidation processes can lead to an increase in the O:C ratio of organic aerosols. These results indicated that aerosol NOCs in HEB were more oxidized aromatics (or aged aromatics), particularly during haze. The average N/C_w ratios of CHON+ and CHON− compounds in HEB (0.13 and 0.15, respectively) (**Table S10**) were higher than those of CHON+ (0.079) and CHON− (0.07) compounds in aerosols directly emitted from coal combustion (Song et al., 2022; Song et al., 2018). The N/C_w ratios were also higher in HEB than in BJ and HZ and increased during hazy days (0.13 for CHON+ and 0.16 for CHON− in hazy days in HEB). It has been suggested that the N/C_w ratio of CHON− compounds tended to increase (from 0.109 to 0.119) after aging of fuel combustion-derived aerosols (Zhao et al., 2022a). Thus, these results, combined with previous analysis of potential precursors for NOCs, suggest that anthropogenic precursor emissions and their atmospheric transformation to form CHON compounds were stronger in HEB than in BJ and HZ. Moreover, considering that the emission intensity of precursors during clean and hazy days may not significantly change, secondary processes may significantly promote the formation of NOCs in HEB during hazy days (the most significant increase in NOC abundance). However, this promoting effect during hazy

405 days was insignificant in BJ and HZ (less increase in NOC abundance).

406

407 **3.3. Main factors influencing aerosol NOC formation in different cities**

408 As discussed in the previous section, the results indicated that AVOCs play a
409 significant role in the formation of NOCs. Furthermore, secondary processes may
410 contribute to NOC formation to varying extents in different cities. This section
411 provides a detailed discussion of the key factors influencing the molecular distribution
412 of NOCs. First, a Spearman correlation analysis was performed to examine the
413 relationship between various parameters and NOCs **(Fig. 3** and **Figs. S8**–**S12**). The
414 peak intensity of most CHON+ compounds (mainly aromatics, as mentioned
415 previously) showed a strong correlation (P < 0.01) with the concentrations of
416 combustion source-related tracers (e.g., SO_2, nss-Cl^-, nss-K^+, CO, and NO_2) (Zhao
417 and Sun, 1986; Streets and Waldhoff, 2000; Shen et al., 2009; Zhang et al., 2011;
418 Mafusire et al., 2016; Liu et al., 2019; Zhang et al., 2021a; Wang et al., 2020) in HEB
419 (**Figs. 3a** and **S8a–d**). Although there was a significant correlation (P < 0.05) between
420 most CHON+ compounds and those combustion source indicators in BJ, the strength
421 of this correlation was weaker in BJ than in HEB (**Figs. 3e** and **S8f–i**). However,
422 similar significant correlations between them were not observed in HZ (**Figs. 3i** and
423 **S8k–n**). Thus, the greatest contribution of anthropogenic activities to the formation of
424 CHON+ compounds in winter was in HEB (central heating with coal), followed by BJ

(central heating with coal and natural gas) and HZ (without central heating). Most of CHN+ and CHON− compounds showed a similar spatial response pattern to those anthropogenic activities (**Figs. S9** and **S10**). These results are consistent with the previous analysis of NOC precursors (**Fig. 2**), which concluded that the intensity of anthropogenic pollutant emissions in different energy consuming cities was an important factor affecting the formation of NOC and causing spatial differences in NOC abundance.

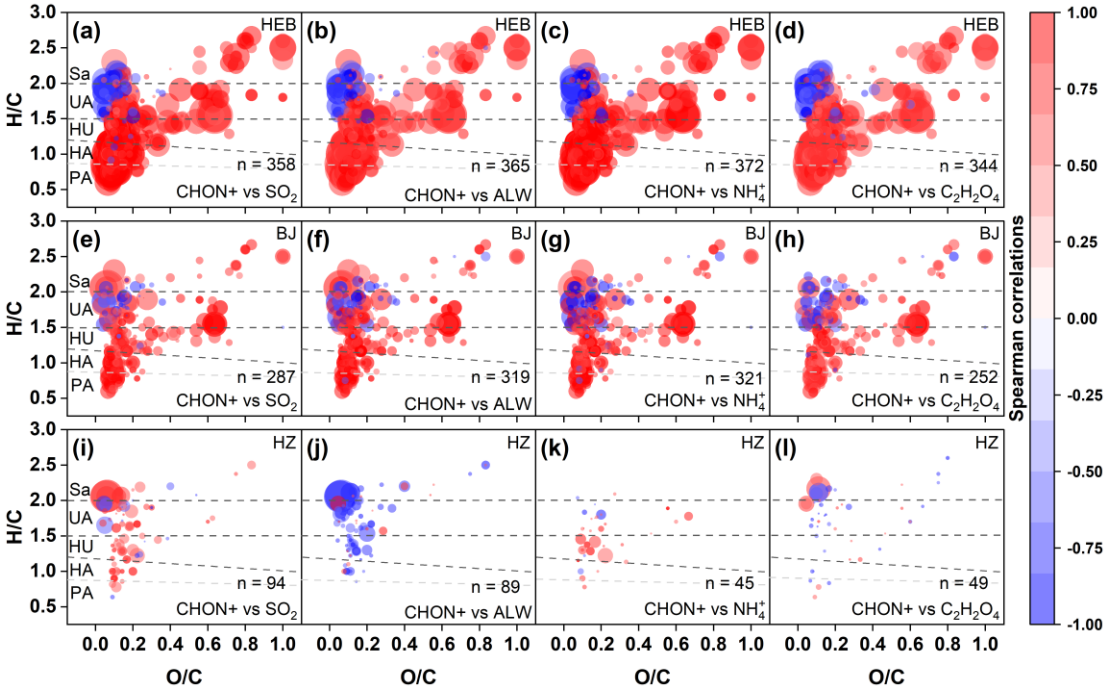

Figure 3. Spearman rank correlation coefficients (with $P < 0.01$ in HEB and $P < 0.05$ in BJ and HZ) of individual CHON+ molecules with selected parameters in (**a**–**d**) HEB, (**e**–**h**) BJ and (**i**–**l**) HZ. The color scale indicates Spearman correlations between the intensity of individual CHON+ molecules and each parameter. The symbol *n* in the bottom right corner of each panel indicates the number of molecular formulas

438 significantly correlated with the variables. The subgroups in the panels include
439 polycyclic aromatic-like (PA), highly aromatic-like (HA), highly unsaturated-like
440 (HU), unsaturated aliphatic-like (UA), and saturated-like (Sa) compounds.
441
442 Furthermore, we found that the peak intensities of most CHON+, CHN+, and
443 CHON− compounds (mainly aromatics) were significantly correlated ($P < 0.01$) with
444 the concentrations of ALW, NH_4^+, oxalic acid, and SO_4^{2-} (**Figs. 3b**–**d**, **S8e**, and
445 **S11**–**S12**) in HEB. The correlations between these NOCs and parameters weakened in
446 BJ and disappeared in HZ (**Figs. 3**, **S8**, and **S11**–**12**). It is generally accepted that
447 SO_4^{2-}, NH_4^+, and NO_3^- in fine aerosols are primarily formed through secondary
448 processes (Gao et al., 2021; Wang et al., 2021d). NH_4^+ can serve as a key reactant in
449 the formation of aerosol NOCs (e.g., "carbonyl-to-imine" transformation) in the
450 aqueous-phase (Laskin et al., 2014; Lee et al., 2013; Li et al., 2019b). Oxalic acid
451 ($C_2H_2O_4$) has been identified as a marker (defined by Nozière et al. (2015)) for
452 aqueous-phase SOA (Xu et al., 2022a; Chen et al., 2021). Additionally, numerous
453 laboratory and field observational studies have shown that ALW can promote the
454 formation of NOCs (Lv et al., 2022; Liu et al., 2023b; Jimenez et al., 2022; Jiang et al.,
455 2023). Thus, these results indicate that aqueous-phase processes can significantly
456 promote the formation of NOCs in HEB, however, as the precursor emission intensity
457 gradually decreased in BJ and HZ, this aqueous-phase promoting effect also

458 decreased.

459 The NMDS analysis between various parameters and NOCs was conducted to
460 further investigate the variations in key factors affecting the formation of NOCs from
461 clean to haze days **(Fig. 4**). The formation of CHON+, CHN+, and CHON−
462 compounds with higher AI_{mod} values (mainly aromatics, as mentioned previously)
463 during haze days in HEB and BJ were closely associated with the factors indicating
464 anthropogenic precursor emissions and aqueous-phase reaction processes. In contrast,
465 the level of oxidants (i.e., O_3 and •OH) played a more important role during clean
466 days in HEB and BJ, driving more highly saturated NOC formation during clean days
467 (**Fig. 4**). A reasonable explanation for this is that the solar radiation and •OH levels on
468 polluted days were lower than those on clean days (**Table S1**). The impacts of various
469 factors on the formation of aerosol NOCs showed a weak discrimination between
470 haze and clean days in HZ (**Fig. 4c, f** and **i**). Laboratory studies have shown that
471 reactive components (e.g., •OH and H_2O_2) in the aqueous phase can continuously
472 convert low-solubility organics to form aqueous phase SOA (Chen et al., 2008; Huang
473 et al., 2011; Dong et al., 2021). Field observations also suggested that precursors
474 (most of them are aromatic compounds) released from the combustion of fossil fuels
475 significantly contributed to the aqueous SOA formation (> 50% total molecules) (Xu
476 et al., 2022a) through the rapid aqueous-phase conversion of primary organic aerosol
477 (POA) to SOA at high RH (Wang et al., 2021a). This implies that higher precursor

abundance can drive more aerosol NOC formation via aqueous-phase processes. As mentioned previously, the emission intensity of precursors decreased sequentially from HEB to BJ and then to HZ. Moreover, the ALW concentrations were much higher on polluted days than on clean days in three investigated cities. The rising ALW during the pollution period and the quiescent steady state of the atmosphere favored the formation of SOA from anthropogenic emission precursors (Guo et al., 2014; He et al., 2018). Thus, the above discussion can suggest that the spatial differences in precursor emission intensity (higher in HEB) and enhancement of aqueous-phase processes in polluted days were the main factors leading to the differences in the proportion (higher in HEB) of increase in NOC abundance from clean days to polluted days in three different energy consuming cities. In addition, the increased VC value (**Table S1**) in clean days (beneficial for the diffusion of pollutants) (Gani et al., 2019) was also an important factor limiting the abundance of NOCs (**Fig. 4**), resulting in a lower NOC abundance on clean days compared to polluted days (**Fig. 1**).

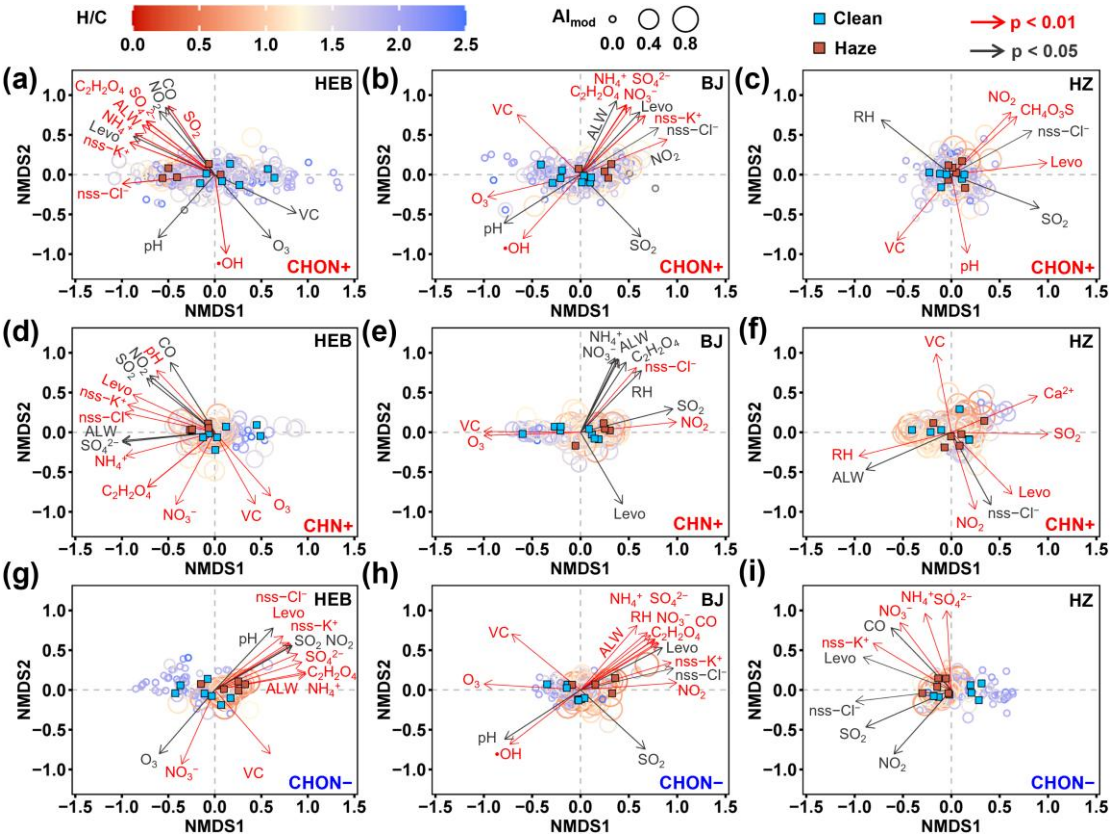

493

494 **Figure 4.** Nonmetric multidimensional scaling of (**a**–**c**) CHON+, (**d**–**f**) CHN+, and

495 (**g**–**i**) CHON− compounds from organic aerosol in different cities. The color and size

496 of the circle indicate the H/C ratio and AI_{mod} value of compounds, respectively.

497 Significant relationships between the variables and ordination (999 permutations) are

498 indicated by $p < 0.05$ (grey) and $p < 0.01$ (red). Insignificant correlations are not

499 shown. The scores of the samples collected during clean and haze periods were shown

500 as blue and brown squares, respectively.

501

502 As mentioned above, the aerosol NOCs of HZ were less affected by

503 anthropogenic pollutants emitted from coal and natural gas combustion compared to

HEB and BJ with centralized heating. Interestingly, we found that the molecular distributions of most aromatic CHON+ compounds in HZ were not only influenced by some anthropogenic pollutants (e.g., SO_2 and NO_2), but also by methanesulfonic acid (CH_4O_3S) (**Fig. 4c**). Moreover, neither CHN+ nor CHON+ exhibited significant correlations with factors related to secondary processes in HZ (**Fig. 4c** and **f**). Methanesulfonic acid has been suggested to be a tracer for ocean aerosols (Ayers and Gras, 1991; Suess et al., 2019). These results suggest that aerosol CHON+ compounds in HZ may be influenced by long-distance transport air masses originating from the ocean. This consideration can be also supported by the fact that only HZ was affected by air masses originated from the ocean (**Fig. S13**). Thus, marine emissions may be an important contributor to aerosol NOCs in HZ, which was significantly different from the cases of HEB and BJ where aromatic pollutants from fossil fuel combustion and aqueous-phase processes control the composition and abundance of aerosol NOCs.

3.4. Potential formation mechanisms of aerosol NOCs in cities with different energy consumption

Figure 5 shows the average signal intensity percentage and signal intensity distributions of NOCs formed by different aqueous-phase processes (**Table S4** and **Figs. S3**–**S5**) in different cities during winter. The identification of specific reaction

pathways was detailed in **Figs. S3**–**S5** and **Sect. S4**. During the entire study period, the cond_N, cond_hy_N, and cond_de_N pathways together accounted for more than 68% (68%−74%) of the total signal intensity of CHON+ compounds in the three cities (**Fig. 5a–c** and **Table S11**). Specifically, the formation of CHON+ compounds was mainly dominated by the cond_N and cond_hy_N pathways in HEB, with less impact from the cond_de_N pathway (**Fig. 5a**). However, CHON+ compounds derived from the cond_de_N pathway showed a much higher proportion in BJ and HZ than in HEB (**Fig. 5b** and **c**). The cond_de_N pathway involves both condensation and dehydration processes (**Table S4 and Fig. S3**). Recent studies have identified that dehydration reactions may occur in aerosols and fog water (Sun et al., 2024), as well as in photochemical transformations of organic compounds in aqueous phase (Lian et al., 2020). While the exact pathways of dehydration reactions in the particle phase remain uncertain, stronger solar radiation in BJ and HZ than in HEB (**Table S1**) may partly explain the higher signal proportion of CHON+ compounds formed through the cond_hy_N pathway in BJ and HZ. Furthermore, the higher signal proportions of CHN+ compounds formed through the de_N pathway in BJ (6%) and HZ (11%) than in HEB (2%) may also be associated with this solar radiation-induced dehydration mechanism (**Fig. 5d–f** and **Table S12**). For CHN+ compounds, the cond_de_N process dominated their formation (**Fig. 5d–f**). In general, the cond_N, cond_hy_N, and cond_de_N processes contributed most significantly to the formation of Re-NOCs

in HEB, followed BJ and HZ.

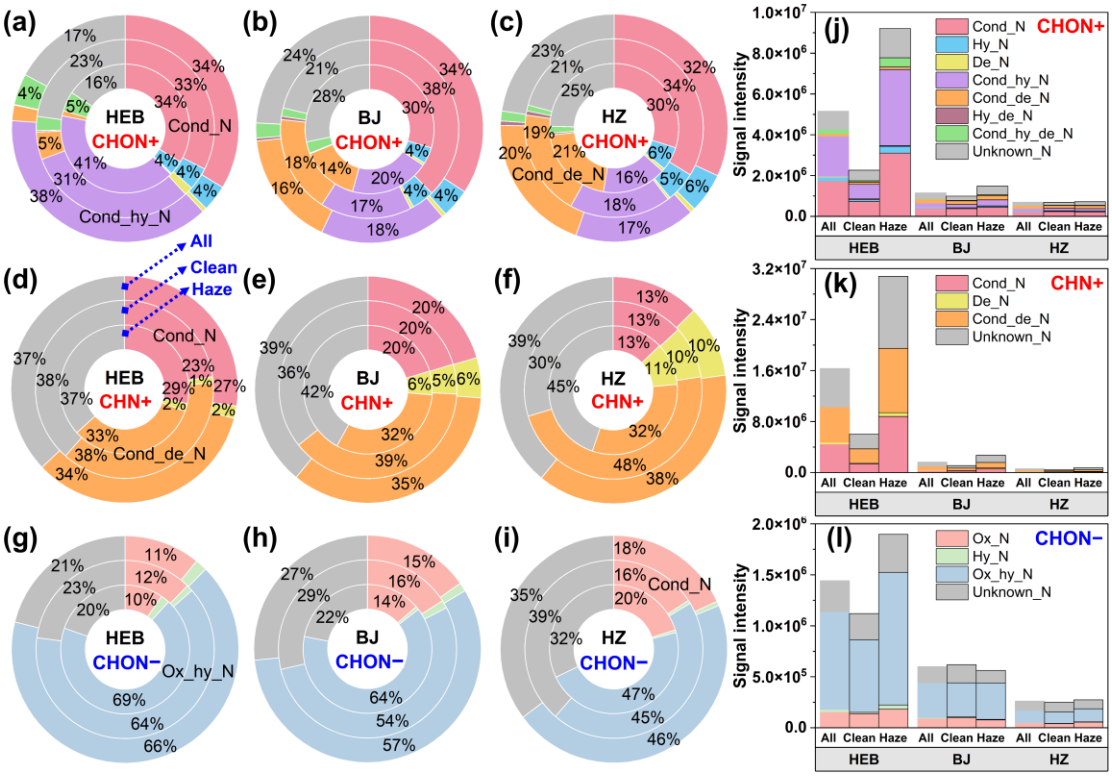

Figure 5. Average percentage distributions of signal intensities for aerosol (**a**–**c**) CHON+, (**d**–**f**) CHN+, and (**g**–**i**) CHON− compounds from various reaction pathways in different cities during winter. Average signal intensity distributions for aerosol (**j**) CHON+, (**k**) CHN+, and (**l**) CHON− compounds from various reaction pathways in different cities during winter.

A typical mechanism for Re-NOC formation is the aqueous-phase reactions between carbonyl compounds and NH_4^+ (or NH_3) (Abudumutailifu et al., 2024; Laskin et al., 2014; Li et al., 2019b; Liu et al., 2023b; Wang et al., 2024). If this mechanism is simplified as a second-order reaction (i.e., [Precursor] + [NH_3 and NH_4^+]

↔ [Re-NOCs]), the production of Re-NOCs is expected to be proportional to the abundances of precursor and NH_4^+ (Yang et al., 2023; Lin et al., 2023). Indeed, the signal intensities of the Re-CHON+ and Re-CHN+ compounds were significantly positively correlated with the signal intensities of their CHO precursors (identified using the precursor-product pairs theory, **Figs. S3** and **S4**) and NH_4^+ concentration in HEB (**Fig. 6a, b, d** and **e**). This correlation gradually weakened from BJ to HZ (**Fig. 6a, b, d** and **e**). As previously discussed, differences in energy consumption patterns resulted in the highest levels of anthropogenic aromatic compound emissions in HEB during the winter, followed by BJ, with the lowest levels in HZ (**Figs. 2** and **S14**). Thus, the signal intensities of CHON+ and CHN+ compounds from cond_N, cond_de_N, and cond_hy_N processes were higher in HEB than in BJ and lowest in HZ (**Fig. 5j** and **k**).

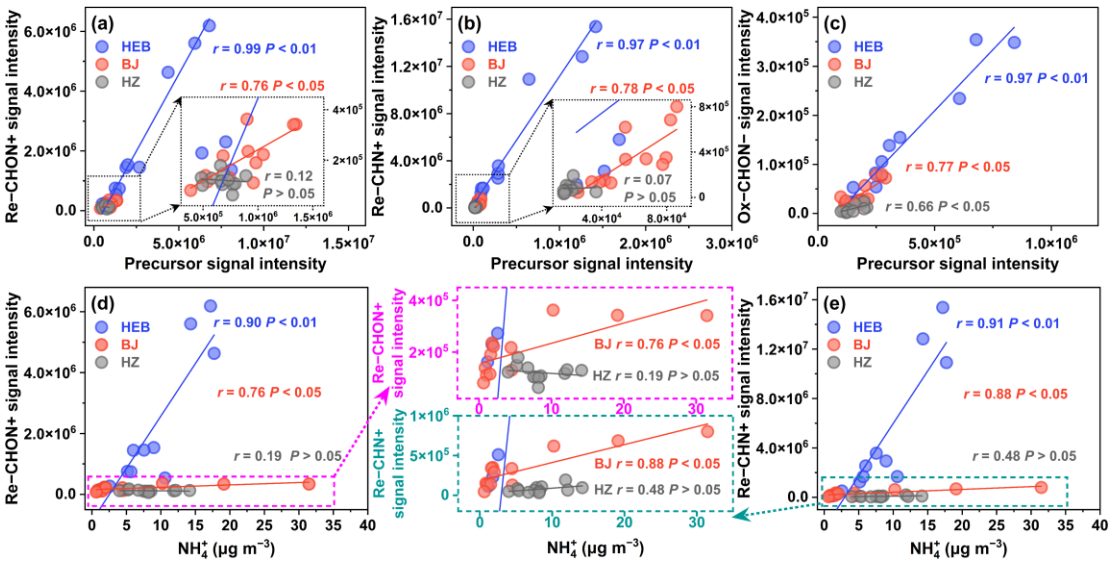

Figure 6. Signal intensity of (**a**) Re-CHON+, (**b**) Re-CHN+, and (**c**) Ox-CHON− compounds as functions of signal intensity of precursors (CHO compounds). Signal

intensity of (**d**) Re-CHON+ and (**e**) Re-CHN+ compounds as functions of the concentrations of NH_4^+.

Additionally, we noticed that the contribution of these aqueous-phase processes to the formation of CHON+ and CHN+ compounds increased significantly from clean to hazy days in HEB and BJ (**Fig. 5**). The increased ALW concentrations (**Table S1**) and atmospheric stability during haze periods likely provided favorable conditions for the precursors to undergo these aqueous-phase reactions, resulting in the formation of NOCs. Clearly, high pollutant emission levels in HEB provided a greater potential to convert precursors into more NOCs via the cond_N, cond_hy_N, and cond_de_N processes during haze periods. Thus, the hazy days in the HEB showed the largest increase in CHON+ and CHN+ compounds from the cond_N, cond_hy_N, and cond_de_N processes (**Fig. 5j** and **k**). In contrast, due to the absence of heating for generally mild winters and the implementation of stricter pollution control measures (more coal usage in HZ than in BJ, as shown in **Fig. 1d**), the precursor emissions in HZ were lower. These emissions were insufficient to support the production of large amounts of NOCs in the aqueous phase. These results also indicate that emission reduction is the key to controlling aerosol NOC pollution.

CHON− compounds derived from the ox_hy_N and ox_N processes together accounted for more than 64% (64%−71%) of the total signal intensity of CHON−

compounds in the three cities (**Fig. 5g–i, l** and **Table S13**). The signal intensity proportions of CHON− compounds formed by the ox_hy_N process in these three cities (ranging from 47% in HZ to 69% in HEB) were higher than that in Wangdu (< 20%) (Jiang et al., 2023). The observation study in Wangdu examined aerosol organic components only in ESI− mode (Jiang et al., 2023), which may underestimate the importance of the CHO+ compounds that could serve as precursors of Ox-NOCs. In general, CHON− compounds formed through the ox_hy_N and ox_N processes showed the highest abundance in HEB, followed by BJ and HZ (**Fig. 5g–i**). According to a simplified reaction mechanism for the formation of Ox-NOCs via aqueous-phase processes (i.e., [Precursor] + [Oxidants] ↔ [Ox-NOCs]) (Shi et al., 2023; Kroflič et al., 2015; Vione et al., 2005), we can infer that Ox-NOCs production is proportional to precursor levels when oxidants (e.g., NO_2 radical or NO_2^+) are in a steady state in the atmosphere. Indeed, the signal intensities of the Ox-CHON− compounds were significantly positively correlated with the signal intensities of their CHO precursors identified using the precursor-product pairs theory in HEB (**Fig. 6c**). Moreover, this correlation gradually weakened from BJ to HZ (**Fig. 6c**). Thus, the spatial differences in the contribution of the ox_hy_N and ox_N processes to Ox-NOC production across the three cities can also be explained by differences in precursor emission intensity, as indicated by above mentioned Re-NOC formation.

4. Conclusion

The abundance, composition, potential precursors, and potential formation mechanisms of NOCs in $PM_{2.5}$ in three Chinese cities with different energy consumption types during the winter were systematically investigated. On average, the total signal intensity of NOCs (i.e., CHN+, CHON+, and CHON− compounds) was highest in HEB, followed by BJ. The lowest total NOC signal intensity was found in HZ. According to the identification of potential precursors of NOCs, we found that anthropogenic aromatic compounds were the main precursors of NOCs during winter in HEB where mainly relies on coal for winter heating, with less impact from BVOCs. Anthropogenic aromatic precursors were also identified to be important contributors to NOC formation in BJ which uses natural gas and coal for winter heating, although the contribution ratio was lower in BJ than in HEB. In contrast, due to generally mild winters resulting in the absence of a winter heating policy and the implementation of strict pollution control measures, as mentioned previously, aromatic precursor emissions in HZ were expected to be the lowest. Furthermore, the NMDS analysis supported that the impact of anthropogenic fossil fuel combustion on NOC pollution gradually decreased from HEB to BJ and then to HZ.

The formation of CHON+ compounds was mainly associated with the cond_N, cond_hy_N, and cond_de_N processes. The cond_N and cond_de_N processes dominated the formation of CHN+ compounds. The production of CHON+ and

CHN+ compounds from the cond_N, cond_hy_N, and cond_de_N processes was highest in HEB, followed by BJ and HZ. The ox_hy_N and ox_N processes contributed significantly to CHON− compound formation, from which the highest CHON− production occurred in HEB and the lowest in HZ. The spatial differences in the contribution of different aqueous-phase processes to NOC production in the three different cities can be attributed to differences in precursor emission intensity. In particular, the contribution of these aqueous-phase processes to the formation of CHON+ and CHN+ compounds showed the most significant increase from clean to hazy days in HEB, followed by BJ. We concluded that high pollutant emission levels can provide a greater potential to convert precursors to produce more NOCs via aqueous-phase processes during haze periods. The above findings are summarized in a diagram (**Fig. 7**).

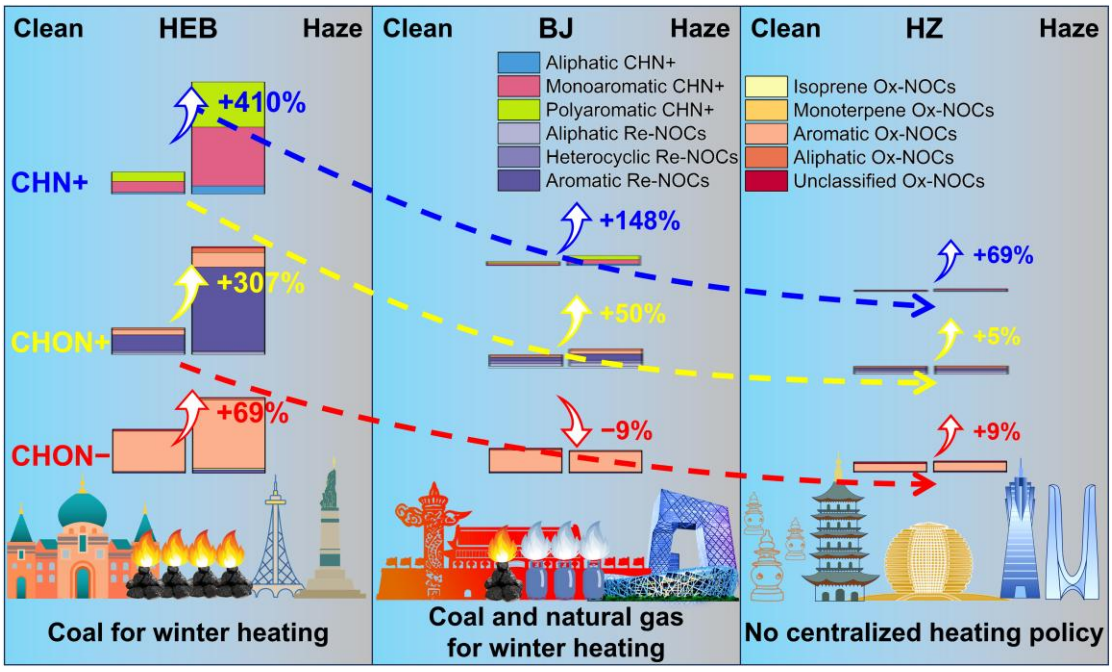

Figure 7. Conceptual illustration showing the characteristics of different NOCs from the clean days to the haze days in different cities.

In general, the aerosol NOCs pollution during winter is closely linked to both the intensity of precursor emissions and the efficiency of aqueous-phase processes in converting these emissions into NOCs. The overall results highlight the importance of emission reduction strategies in controlling aerosol NOCs pollution during winter. It is imperative to manage precursor emissions during hazy episodes in order to restrict the increased formation of secondary NOCs in conditions of high humidity. Moreover, targeted reduction of precursor emissions, especially from coal combustion, could significantly mitigate NOCs levels, thereby improving air quality and public health in urban areas. The transition to cleaner energy sources, as evidenced by the decreased gradient of NOC pollution from HEB to BJ to HZ, represents an effective pathway for the mitigation of NOC pollution. Future research should focus on further elucidating the specific pathways of aqueous-phase NOC formation and developing available models to predict NOC dynamics under varying environmental conditions. Additionally, research into the long-term effects of transitioning to cleaner energy sources on the reduction of NOC pollution will be essential for guiding effective air quality management strategies.

Data availability. The data presented in this work are available upon request from the

corresponding authors.

Competing interests. The authors declare no conflicts of interest relevant to this study.

Supplement. Details of parameter calculation, classification method for identifying precursors of NOCs, classification of possible aqueous-phase processes NOCs based on precursor-product pairs, thirteen tables (Tables S1−S13), and fourteen extensive figures (Figures S1−S14) are provided in the Supplement.

Author contributions. YX designed the study. YJM, TY, LG, HX, and HWX performed field measurements and sample collection; YJM performed chemical analysis; YX and YJM performed data analysis; YX and YJM wrote the original manuscript; and YX, YJM, and HYX reviewed and edited the manuscript.

Financial support. This study was kindly supported by the National Natural Science Foundation of China through grant 42303081, Shanghai “Science and Technology Innovation Action Plan” Shanghai Sailing Program through grant 22YF1418700, and the National Key Research and Development Program of China through gran 2023YFF0806001

References

Abudumutailifu, M., Shang, X., Wang, L., Zhang, M., Kang, H., Chen, Y., Li, L., Ju, R., Li, B., Ouyang, H., Tang, X., Li, C., Wang, L., Wang, X., George, C., Rudich, Y., Zhang, R., and Chen, J.: Unveiling the Molecular Characteristics, Origins, and Formation Mechanism of Reduced Nitrogen Organic Compounds in the Urban Atmosphere of Shanghai Using a Versatile Aerosol Concentration Enrichment System, Environ. Sci. Technol., 10.1021/acs.est.3c04071, 2024.

Arimoto, R., Duce, R. A., Savoie, D. L., Prospero, J. M., Talbot, R., Cullen, J. D., Tomza, U., Lewis, N. F., and Ray, B. J.: Relationships among aerosol constituents from Asia and the North Pacific during PEM-West A, J. Geophys. Res.-Atmos., 101, 2011-2023, https://doi.org/10.1029/95JD01071, 1996.

Ayers, G. P. and Gras, J. L.: Seasonal relationship between cloud condensation nuclei and aerosol methanesulphonate in marine air, Nature, 353, 834-835, 10.1038/353834a0, 1991.

Bond, T. C., Wehner, B., Plewka, A., Wiedensohler, A., Heintzenberg, J., and Charlson, R. J.: Climate-relevant properties of primary particulate emissions from oil and natural gas combustion, Atmos. Environ., 40, 3574-3587, https://doi.org/10.1016/j.atmosenv.2005.12.030, 2006.

Cape, J. N., Cornell, S. E., Jickells, T. D., and Nemitz, E.: Organic nitrogen in

the atmosphere — Where does it come from? A review of sources and methods, Atmos. Res., 102, 30-48, https://doi.org/10.1016/j.atmosres.2011.07.009, 2011.

Chao, A., Chazdon, R. L., Colwell, R. K., and Shen, T.-J.: Abundance-Based Similarity Indices and Their Estimation When There Are Unseen Species in Samples, Biometrics, 62, 361-371, https://doi.org/10.1111/j.1541-0420.2005.00489.x, 2006.

Chen, Y., Guo, H., Nah, T., Tanner, D. J., Sullivan, A. P., Takeuchi, M., Gao, Z., Vasilakos, P., Russell, A. G., Baumann, K., Huey, L. G., Weber, R. J., and Ng, N. L.: Low-Molecular-Weight Carboxylic Acids in the Southeastern U.S.: Formation, Partitioning, and Implications for Organic Aerosol Aging, Environ. Sci. Technol., 55, 6688-6699, 10.1021/acs.est.1c01413, 2021.

Chen, Z. M., Wang, H. L., Zhu, L. H., Wang, C. X., Jie, C. Y., and Hua, W.: Aqueous-phase ozonolysis of methacrolein and methyl vinyl ketone: a potentially important source of atmospheric aqueous oxidants, Atmos. Chem. Phys., 8, 2255-2265, 10.5194/acp-8-2255-2008, 2008.

Ditto, J. C., Machesky, J., and Gentner, D. R.: Analysis of reduced and oxidized nitrogen-containing organic compounds at a coastal site in summer and winter, Atmos. Chem. Phys., 22, 3045-3065, https://doi.org/10.5194/acp-22-3045-2022, 2022.

Dong, P., Chen, Z., Qin, X., and Gong, Y.: Water Significantly Changes the Ring-Cleavage Process During Aqueous Photooxidation of Toluene, Environ. Sci. Technol., 55, 16316-16325, 10.1021/acs.est.1c04770, 2021.

Ehhalt, D. H. and Rohrer, F.: Dependence of the OH concentration on solar UV, J. Geophys. Res.-Atmos., 105, 3565-3571, https://doi.org/10.1029/1999JD901070, 2000.

Gani, S., Bhandari, S., Seraj, S., Wang, D. S., Patel, K., Soni, P., Arub, Z., Habib, G., Hildebrandt Ruiz, L., and Apte, J. S.: Submicron aerosol composition in the world's most polluted megacity: the Delhi Aerosol Supersite study, Atmos. Chem. Phys., 19, 6843-6859, 10.5194/acp-19-6843-2019, 2019.

Gao, J., Li, Y., Li, J., Shi, G., Liu, Z., Han, B., Tian, X., Wang, Y., Feng, Y., and Russell, A. G.: Impact of Formation Pathways on Secondary Inorganic Aerosol During Haze Pollution in Beijing: Quantitative Evidence From High-Resolution Observation and Modeling, Geophys. Res. Lett., 48, e2021GL095623, https://doi.org/10.1029/2021GL095623, 2021.

Gui, L., Xu, Y., You, Y.-C., Ma, Y.-J., Yang, T., Liu, T., Xiao, H.-W., Xiao, H., and Xiao, H.-Y.: Oxidative Degradation of Higher-Molecular-Weight Aromatic Amine Compounds Is a Potential Source of Anilinium in Urban Aerosols, Environ. Sci. Technol. Lett., 11, 1355-1361, 10.1021/acs.estlett.4c00935, 2024.

Guo, S., Hu, M., Zamora, M. L., Peng, J., Shang, D., Zheng, J., Du, Z., Wu, Z., Shao, M., Zeng, L., Molina, M. J., and Zhang, R.: Elucidating severe urban haze formation in China, P. Natl. Acad. Sci. USA, 111, 17373-17378, doi:10.1073/pnas.1419604111, 2014.

Guo, Y., Yan, C., Liu, Y., Qiao, X., Zheng, F., Zhang, Y., Zhou, Y., Li, C., Fan, X.,

744 Lin, Z., Feng, Z., Zhang, Y., Zheng, P., Tian, L., Nie, W., Wang, Z., Huang, D.,
745 Daellenbach, K. R., Yao, L., Dada, L., Bianchi, F., Jiang, J., Liu, Y., Kerminen, V. M.,
746 and Kulmala, M.: Seasonal variation in oxygenated organic molecules in urban
747 Beijing and their contribution to secondary organic aerosol, Atmos. Chem. Phys., 22,
748 10077-10097, 10.5194/acp-22-10077-2022, 2022.
749 Hallquist, M., Wenger, J. C., Baltensperger, U., Rudich, Y., Simpson, D., Claeys,
750 M., Dommen, J., Donahue, N. M., George, C., Goldstein, A. H., Hamilton, J. F.,
751 Herrmann, H., Hoffmann, T., Iinuma, Y., Jang, M., Jenkin, M. E., Jimenez, J. L.,
752 Kiendler-Scharr, A., Maenhaut, W., McFiggans, G., Mentel, T. F., Monod, A., Prévôt,
753 A. S. H., Seinfeld, J. H., Surratt, J. D., Szmigielski, R., and Wildt, J.: The formation,
754 properties and impact of secondary organic aerosol: current and emerging issues,
755 Atmos. Chem. Phys., 9, 5155-5236, 10.5194/acp-9-5155-2009, 2009.
756 Han, Y., Zhang, X., Li, L., Lin, Y., Zhu, C., Zhang, N., Wang, Q., and Cao, J.:
757 Enhanced Production of Organosulfur Species during a Severe Winter Haze Episode
758 in the Guanzhong Basin of Northwest China, Environ. Sci. Technol.,
759 https://doi.org/10.1021/acs.est.3c02914, 2023.
760 He, C., Che, H., Bao, Z., Liu, Y., Li, Q., Hu, M., Zhou, J., Zhang, S., Yao, X., Shi,
761 Q., Chen, C., Han, Y., Meng, L., Long, X., Yang, F., and Chen, Y.: Evolution of
762 nucleophilic high molecular-weight organic compounds in ambient aerosols: a case
763 study, Atmos. Chem. Phys., 24, 1627-1639, 10.5194/acp-24-1627-2024, 2024.

764 He, Q.-F., Ding, X., Fu, X.-X., Zhang, Y.-Q., Wang, J.-Q., Liu, Y.-X., Tang, M.-J.,
765 Wang, X.-M., and Rudich, Y.: Secondary Organic Aerosol Formation From Isoprene
766 Epoxides in the Pearl River Delta, South China: IEPOX- and HMML-Derived Tracers,
767 J. Geophys. Res.-Atmos., 123, 6999-7012, https://doi.org/10.1029/2017JD028242,
768 2018.
769 Heald, C. L., Kroll, J. H., Jimenez, J. L., Docherty, K. S., DeCarlo, P. F., Aiken,
770 A. C., Chen, Q., Martin, S. T., Farmer, D. K., and Artaxo, P.: A simplified description
771 of the evolution of organic aerosol composition in the atmosphere, Geophys. Res.
772 Lett., 37, https://doi.org/10.1029/2010GL042737, 2010.
773 Hodas, N., Sullivan, A. P., Skog, K., Keutsch, F. N., Collett, J. L., Jr., Decesari,
774 S., Facchini, M. C., Carlton, A. G., Laaksonen, A., and Turpin, B. J.: Aerosol Liquid
775 Water Driven by Anthropogenic Nitrate: Implications for Lifetimes of Water-Soluble
776 Organic Gases and Potential for Secondary Organic Aerosol Formation, Environ. Sci.
777 Technol., 48, 11127-11136, 10.1021/es5025096, 2014.
778 Huang, D., Zhang, X., Chen, Z. M., Zhao, Y., and Shen, X. L.: The kinetics and
779 mechanism of an aqueous phase isoprene reaction with hydroxyl radical, Atmos.
780 Chem. Phys., 11, 7399-7415, 10.5194/acp-11-7399-2011, 2011.
781 Huang, S., Shen, Z., Yang, X., Bai, G., Zhang, L., Zeng, Y., Sun, J., Xu, H., Ho,
782 S. S. H., Zhang, Y., and Cao, J.: Nitroaromatic compounds in six major Chinese cities:
783 Influence of different formation mechanisms on light absorption properties, Sci. Total

784 Environ., 930, 172672, https://doi.org/10.1016/j.scitotenv.2024.172672, 2024.

785 Jiang, H., Li, J., Tang, J., Zhao, S., Chen, Y., Tian, C., Zhang, X., Jiang, B., Liao,
786 Y., and Zhang, G.: Factors Influencing the Molecular Compositions and Distributions
787 of Atmospheric Nitrogen-Containing Compounds, J. Geophys. Res.-Atmos., 127,
788 e2021JD036284, https://doi.org/10.1029/2021JD036284, 2022.

789 Jiang, H., Cai, J., Feng, X., Chen, Y., Wang, L., Jiang, B., Liao, Y., Li, J., Zhang,
790 G., Mu, Y., and Chen, J.: Aqueous-Phase Reactions of Anthropogenic Emissions Lead
791 to the High Chemodiversity of Atmospheric Nitrogen-Containing Compounds during
792 the Haze Event, Environ. Sci. Technol., 57, 16500-16511, 10.1021/acs.est.3c06648,
793 2023.

794 Jimenez, N. G., Sharp, K. D., Gramyk, T., Ugland, D. Z., Tran, M.-K., Rojas, A.,
795 Rafla, M. A., Stewart, D., Galloway, M. M., Lin, P., Laskin, A., Cazaunau, M., Pangui,
796 E., Doussin, J.-F., and De Haan, D. O.: Radical-Initiated Brown Carbon Formation in
797 Sunlit Carbonyl–Amine–Ammonium Sulfate Mixtures and Aqueous Aerosol Particles,
798 ACS Earth Space Chem., 6, 228-238, 10.1021/acsearthspacechem.1c00395, 2022.

799 Kellerman, A. M., Dittmar, T., Kothawala, D. N., and Tranvik, L. J.:
800 Chemodiversity of dissolved organic matter in lakes driven by climate and hydrology,
801 Nature Communications, 5, 3804, 10.1038/ncomms4804, 2014.

802 Koch, B. P. and Dittmar, T.: From mass to structure: an aromaticity index for
803 high-resolution mass data of natural organic matter, Rapid Commun. Mass Spectrom.,

804 20, 926-932, https://doi.org/10.1002/rcm.2386, 2006.

805 Kroflič, A., Grilc, M., and Grgić, I.: Does toxicity of aromatic pollutants increase
806 under remote atmospheric conditions?, Scientific Reports, 5, 8859,
807 10.1038/srep08859, 2015.

808 Kroll, J. H., Donahue, N. M., Jimenez, J. L., Kessler, S. H., Canagaratna, M. R.,
809 Wilson, K. R., Altieri, K. E., Mazzoleni, L. R., Wozniak, A. S., Bluhm, H., Mysak, E.
810 R., Smith, J. D., Kolb, C. E., and Worsnop, D. R.: Carbon oxidation state as a metric
811 for describing the chemistry of atmospheric organic aerosol, Nat. Chem., 3, 133-139,
812 https://doi.org/10.1038/nchem.948, 2011.

813 Křůmal, K., Mikuška, P., Horák, J., Hopan, F., and Krpec, K.: Comparison of
814 emissions of gaseous and particulate pollutants from the combustion of biomass and
815 coal in modern and old-type boilers used for residential heating in the Czech Republic,
816 Central Europe, Chemosphere, 229, 51-59,
817 https://doi.org/10.1016/j.chemosphere.2019.04.137, 2019.

818 Kuwata, M. and Martin, S. T.: Phase of atmospheric secondary organic material
819 affects its reactivity, P. Natl. Acad. Sci. USA, 109, 17354-17359,
820 doi:10.1073/pnas.1209071109, 2012.

821 Laskin, J., Laskin, A., Nizkorodov, S. A., Roach, P., Eckert, P., Gilles, M. K.,
822 Wang, B., Lee, H. J., and Hu, Q.: Molecular Selectivity of Brown Carbon
823 Chromophores, Environ. Sci. Technol., 48, 12047-12055,

https://doi.org/10.1021/es503432r, 2014.

Lee, A. K. Y., Zhao, R., Li, R., Liggio, J., Li, S.-M., and Abbatt, J. P. D.: Formation of Light Absorbing Organo-Nitrogen Species from Evaporation of Droplets Containing Glyoxal and Ammonium Sulfate, Environ. Sci. Technol., 47, 12819-12826, 10.1021/es402687w, 2013.

Li, X., Song, S., Zhou, W., Hao, J., Worsnop, D. R., and Jiang, J.: Interactions between aerosol organic components and liquid water content during haze episodes in Beijing, Atmos. Chem. Phys., 19, 12163-12174, 10.5194/acp-19-12163-2019, 2019a.

Li, Y., Fu, T.-M., Yu, J. Z., Yu, X., Chen, Q., Miao, R., Zhou, Y., Zhang, A., Ye, J., Yang, X., Tao, S., Liu, H., and Yao, W.: Dissecting the contributions of organic nitrogen aerosols to global atmospheric nitrogen deposition and implications for ecosystems, National Science Review, 10, 10.1093/nsr/nwad244, 2023.

Li, Z., Nizkorodov, S. A., Chen, H., Lu, X., Yang, X., and Chen, J.: Nitrogen-containing secondary organic aerosol formation by acrolein reaction with ammonia/ammonium, Atmos. Chem. Phys., 19, 1343-1356, 10.5194/acp-19-1343-2019, 2019b.

Lian, L., Yan, S., Zhou, H., and Song, W.: Overview of the Phototransformation of Wastewater Effluents by High-Resolution Mass Spectrometry, Environ. Sci. Technol., 54, 1816-1826, 10.1021/acs.est.9b04669, 2020.

Lin, X., Xu, Y., Zhu, R.-G., Xiao, H.-W., and Xiao, H.-Y.: Proteinaceous Matter

in $PM_{2.5}$ in Suburban Guiyang, Southwestern China: Decreased Importance in Long-Range Transport and Atmospheric Degradation, J. Geophys. Res.-Atmos., 128, e2023JD038516, https://doi.org/10.1029/2023JD038516, 2023.

Liu, T., Xu, Y., Sun, Q.-B., Xiao, H.-W., Zhu, R.-G., Li, C.-X., Li, Z.-Y., Zhang, K.-Q., Sun, C.-X., and Xiao, H.-Y.: Characteristics, Origins, and Atmospheric Processes of Amines in Fine Aerosol Particles in Winter in China, J. Geophys. Res.-Atmos., 128, e2023JD038974, https://doi.org/10.1029/2023JD038974, 2023a.

Liu, X.-Y., He, K.-B., Zhang, Q., Lu, Z.-F., Wang, S.-W., Zhang, Y.-X., and Streets, D. G.: Analysis of the origins of black carbon and carbon monoxide transported to Beijing, Tianjin, and Hebei in China, Sci. Total Environ., 653, 1364-1376, https://doi.org/10.1016/j.scitotenv.2018.09.274, 2019.

Liu, X., Wang, H., Wang, F., Lv, S., Wu, C., Zhao, Y., Zhang, S., Liu, S., Xu, X., Lei, Y., and Wang, G.: Secondary Formation of Atmospheric Brown Carbon in China Haze: Implication for an Enhancing Role of Ammonia, Environ. Sci. Technol., 57, 11163-11172, 10.1021/acs.est.3c03948, 2023b.

Liu, Y., Nie, W., Li, Y., Ge, D., Liu, C., Xu, Z., Chen, L., Wang, T., Wang, L., Sun, P., Qi, X., Wang, J., Xu, Z., Yuan, J., Yan, C., Zhang, Y., Huang, D., Wang, Z., Donahue, N. M., Worsnop, D., Chi, X., Ehn, M., and Ding, A.: Formation of condensable organic vapors from anthropogenic and biogenic volatile organic compounds (VOCs) is strongly perturbed by NOx in eastern China, Atmos. Chem.

Phys., 21, 14789-14814, 10.5194/acp-21-14789-2021, 2021.

Liu, Z., Zhu, B., Zhu, C., Ruan, T., Li, J., Chen, H., Li, Q., Wang, X., Wang, L., Mu, Y., Collett, J., George, C., Wang, Y., Wang, X., Su, J., Yu, S., Mellouki, A., Chen, J., and Jiang, G.: Abundant nitrogenous secondary organic aerosol formation accelerated by cloud processing, iScience, 26, 108317, https://doi.org/10.1016/j.isci.2023.108317, 2023c.

Lv, S., Wang, F., Wu, C., Chen, Y., Liu, S., Zhang, S., Li, D., Du, W., Zhang, F., Wang, H., Huang, C., Fu, Q., Duan, Y., and Wang, G.: Gas-to-Aerosol Phase Partitioning of Atmospheric Water-Soluble Organic Compounds at a Rural Site in China: An Enhancing Effect of NH_3 on SOA Formation, Environ. Sci. Technol., 56, 3915-3924, 10.1021/acs.est.1c06855, 2022.

Ma, L., Li, B., Liu, Y., Sun, X., Fu, D., Sun, S., Thapa, S., Geng, J., Qi, H., Zhang, A., and Tian, C.: Characterization, sources and risk assessment of $PM_{2.5}$-bound polycyclic aromatic hydrocarbons (PAHs) and nitrated PAHs (NPAHs) in Harbin, a cold city in Northern China, Journal of Cleaner Production, 264, 121673, https://doi.org/10.1016/j.jclepro.2020.121673, 2020.

Ma, Y. J., Xu, Y., Yang, T., Xiao, H. W., and Xiao, H. Y.: Measurement report: Characteristics of nitrogen-containing organics in $PM_{2.5}$ in Ürümqi, northwestern China – differential impacts of combustion of fresh and aged biomass materials, Atmos. Chem. Phys., 24, 4331-4346, 10.5194/acp-24-4331-2024, 2024.

884 Mafusire, G., Annegarn, H. J., Vakkari, V., Beukes, J. P., Josipovic, M., van Zyl,
885 P. G., and Laakso, L.: Submicrometer aerosols and excess CO as tracers for biomass
886 burning air mass transport over southern Africa, J. Geophys. Res.-Atmos., 121,
887 10,262-210,282, https://doi.org/10.1002/2015JD023965, 2016.
888 MEEPRC: Technical Regulation on Ambient Air Quality Index (on trial): HJ
889 633—2012, Ministry of Ecology and Environment of the People's Republic of China,
890 https://www.mee.gov.cn/ywgz/fgbz/bz/bzwb/jcffbz/201203/t20120302_224166.shtml,
891 (last access: 10 December 2024), 2012.
892 Montoya-Aguilera, J., Hinks, M. L., Aiona, P. K., Wingen, L. M., Horne, J. R.,
893 Zhu, S., Dabdub, D., Laskin, A., Laskin, J., Lin, P., and Nizkorodov, S. A.: Reactive
894 Uptake of Ammonia by Biogenic and Anthropogenic Organic Aerosols, in:
895 Multiphase Environmental Chemistry in the Atmosphere, ACS Symposium Series,
896 1299, American Chemical Society, 127-147, doi:10.1021/bk-2018-1299.ch007
897 10.1021/bk-2018-1299.ch007, 2018.
898 Ng, N. L., Brown, S. S., Archibald, A. T., Atlas, E., Cohen, R. C., Crowley, J. N.,
899 Day, D. A., Donahue, N. M., Fry, J. L., Fuchs, H., Griffin, R. J., Guzman, M. I.,
900 Herrmann, H., Hodzic, A., Iinuma, Y., Jimenez, J. L., Kiendler-Scharr, A., Lee, B. H.,
901 Luecken, D. J., Mao, J., McLaren, R., Mutzel, A., Osthoff, H. D., Ouyang, B.,
902 Picquet-Varrault, B., Platt, U., Pye, H. O. T., Rudich, Y., Schwantes, R. H., Shiraiwa,
903 M., Stutz, J., Thornton, J. A., Tilgner, A., Williams, B. J., and Zaveri, R. A.: Nitrate

radicals and biogenic volatile organic compounds: oxidation, mechanisms, and organic aerosol, Atmos. Chem. Phys., 17, 2103-2162, 10.5194/acp-17-2103-2017, 2017.

Nguyen, T. B., Bates, K. H., Crounse, J. D., Schwantes, R. H., Zhang, X., Kjaergaard, H. G., Surratt, J. D., Lin, P., Laskin, A., Seinfeld, J. H., and Wennberg, P. O.: Mechanism of the hydroxyl radical oxidation of methacryloyl peroxynitrate (MPAN) and its pathway toward secondary organic aerosol formation in the atmosphere, Phys. Chem. Chem. Phys., 17, 17914-17926, https://doi.org/10.1039/C5CP02001H, 2015.

Nie, W., Yan, C., Huang, D. D., Wang, Z., Liu, Y., Qiao, X., Guo, Y., Tian, L., Zheng, P., Xu, Z., Li, Y., Xu, Z., Qi, X., Sun, P., Wang, J., Zheng, F., Li, X., Yin, R., Dallenbach, K. R., Bianchi, F., Petäjä, T., Zhang, Y., Wang, M., Schervish, M., Wang, S., Qiao, L., Wang, Q., Zhou, M., Wang, H., Yu, C., Yao, D., Guo, H., Ye, P., Lee, S., Li, Y. J., Liu, Y., Chi, X., Kerminen, V.-M., Ehn, M., Donahue, N. M., Wang, T., Huang, C., Kulmala, M., Worsnop, D., Jiang, J., and Ding, A.: Secondary organic aerosol formed by condensing anthropogenic vapours over China's megacities, Nature Geoscience, 15, 255-261, 10.1038/s41561-022-00922-5, 2022.

Nozière, B., Kalberer, M., Claeys, M., Allan, J., D'Anna, B., Decesari, S., Finessi, E., Glasius, M., Grgić, I., Hamilton, J. F., Hoffmann, T., Iinuma, Y., Jaoui, M., Kahnt, A., Kampf, C. J., Kourtchev, I., Maenhaut, W., Marsden, N., Saarikoski, S.,

924 Schnelle-Kreis, J., Surratt, J. D., Szidat, S., Szmigielski, R., and Wisthaler, A.: The
925 Molecular Identification of Organic Compounds in the Atmosphere: State of the Art
926 and Challenges, Chem. Rev., 115, 3919-3983, 10.1021/cr5003485, 2015.
927 Oksanen, J., Kindt, R., Legendre, P., O'Hara, B., Stevens, M. H. H., Oksanen, M.
928 J., and Suggests, M.: The vegan package, Community ecology package, 10, 719, 2007.
929 Perraud, V., Bruns, E. A., Ezell, M. J., Johnson, S. N., Yu, Y., Alexander, M. L.,
930 Zelenyuk, A., Imre, D., Chang, W. L., Dabdub, D., Pankow, J. F., and Finlayson-Pitts,
931 B. J.: Nonequilibrium atmospheric secondary organic aerosol formation and growth, P.
932 Natl. Acad. Sci. USA, 109, 2836-2841, doi:10.1073/pnas.1119909109, 2012.
933 Rollins, A. W., Browne, E. C., Min, K.-E., Pusede, S. E., Wooldridge, P. J.,
934 Gentner, D. R., Goldstein, A. H., Liu, S., Day, D. A., Russell, L. M., and Cohen, R. C.:
935 Evidence for NO_x Control over Nighttime SOA Formation, Science, 337, 1210-1212,
936 https://doi.org/10.1126/science.1221520, 2012.
937 Shen, Z., Cao, J., Arimoto, R., Han, Z., Zhang, R., Han, Y., Liu, S., Okuda, T.,
938 Nakao, S., and Tanaka, S.: Ionic composition of TSP and $PM_{2.5}$ during dust storms
939 and air pollution episodes at Xi'an, China, Atmos. Environ., 43, 2911-2918,
940 https://doi.org/10.1016/j.atmosenv.2009.03.005, 2009.
941 Shi, X., Qiu, X., Cheng, Z., Chen, Q., Rudich, Y., and Zhu, T.: Isomeric
942 Identification of Particle-Phase Organic Nitrates through Gas Chromatography and
943 Time-of-Flight Mass Spectrometry Coupled with an Electron Capture Negative

944 Ionization Source, Environ. Sci. Technol., 54, 707-713, 10.1021/acs.est.9b05818,
945 2020.
946 Shi, X., Qiu, X., Li, A., Jiang, X., Wei, G., Zheng, Y., Chen, Q., Chen, S., Hu, M.,
947 Rudich, Y., and Zhu, T.: Polar Nitrated Aromatic Compounds in Urban Fine
948 Particulate Matter: A Focus on Formation via an Aqueous-Phase Radical Mechanism,
949 Environ. Sci. Technol., 57, 5160-5168, 10.1021/acs.est.2c07324, 2023.
950 Singh, S. and Kumar, R.: Air Pollution and Its Associated Impacts on
951 Atmosphere and Biota Health, in: Extremes in Atmospheric Processes and
952 Phenomenon: Assessment, Impacts and Mitigation, edited by: Saxena, P., Shukla, A.,
953 and Gupta, A. K., Springer Nature Singapore, Singapore, 29-58, 10.1007/978-981-16-
954 7727-4_3, 2022.
955 Song, J., Li, M., Jiang, B., Wei, S., Fan, X., and Peng, P. a.: Molecular
956 Characterization of Water-Soluble Humic like Substances in Smoke Particles Emitted
957 from Combustion of Biomass Materials and Coal Using Ultrahigh-Resolution
958 Electrospray Ionization Fourier Transform Ion Cyclotron Resonance Mass
959 Spectrometry, Environ. Sci. Technol., 52, 2575-2585,
960 https://doi.org/10.1021/acs.est.7b06126, 2018.
961 Song, J., Li, M., Zou, C., Cao, T., Fan, X., Jiang, B., Yu, Z., Jia, W., and Peng, P.
962 a.: Molecular Characterization of Nitrogen-Containing Compounds in Humic-like
963 Substances Emitted from Biomass Burning and Coal Combustion, Environ. Sci.

964 Technol., 56, 119-130, https://doi.org/10.1021/acs.est.1c04451, 2022.

965 Stockwell, C. E., Veres, P. R., Williams, J., and Yokelson, R. J.: Characterization
966 of biomass burning emissions from cooking fires, peat, crop residue, and other fuels
967 with high-resolution proton-transfer-reaction time-of-flight mass spectrometry, Atmos.
968 Chem. Phys., 15, 845-865, 10.5194/acp-15-845-2015, 2015.

969 Streets, D. G. and Waldhoff, S. T.: Present and future emissions of air pollutants
970 in China:: SO_2, NO_x, and CO, Atmos. Environ., 34, 363-374,
971 https://doi.org/10.1016/S1352-2310(99)00167-3, 2000.

972 Su, S., Xie, Q., Lang, Y., Cao, D., Xu, Y., Chen, J., Chen, S., Hu, W., Qi, Y., Pan,
973 X., Sun, Y., Wang, Z., Liu, C.-Q., Jiang, G., and Fu, P.: High Molecular Diversity of
974 Organic Nitrogen in Urban Snow in North China, Environ. Sci. Technol., 55, 4344-
975 4356, https://dx.doi.org/10.1021/acs.est.0c06851, 2021.

976 Suess, E., Aemisegger, F., Sonke, J. E., Sprenger, M., Wernli, H., and Winkel, L.
977 H. E.: Marine versus Continental Sources of Iodine and Selenium in Rainfall at Two
978 European High-Altitude Locations, Environ. Sci. Technol., 53, 1905-1917,
979 10.1021/acs.est.8b05533, 2019.

980 Sun, W., Hu, X., Fu, Y., Zhang, G., Zhu, Y., Wang, X., Yan, C., Xue, L., Meng,
981 H., Jiang, B., Liao, Y., Wang, X., Peng, P., and Bi, X.: Different formation pathways
982 of nitrogen-containing organic compounds in aerosols and fog water in northern
983 China, Atmos. Chem. Phys., 24, 6987-6999, 10.5194/acp-24-6987-2024, 2024.

Surratt, J. D., Chan, A. W. H., Eddingsaas, N. C., Chan, M., Loza, C. L., Kwan, A. J., Hersey, S. P., Flagan, R. C., Wennberg, P. O., and Seinfeld, J. H.: Reactive intermediates revealed in secondary organic aerosol formation from isoprene, P. Natl. Acad. Sci. USA, 107, 6640-6645, doi:10.1073/pnas.0911114107, 2010.

Vione, D., Maurino, V., Minero, C., and Pelizzetti, E.: Aqueous Atmospheric Chemistry: Formation of 2,4-Dinitrophenol upon Nitration of 2-Nitrophenol and 4-Nitrophenol in Solution, Environ. Sci. Technol., 39, 7921-7931, 10.1021/es050824m, 2005.

Vu, T. V., Shi, Z., Cheng, J., Zhang, Q., He, K., Wang, S., and Harrison, R. M.: Assessing the impact of clean air action on air quality trends in Beijing using a machine learning technique, Atmos. Chem. Phys., 19, 11303-11314, 10.5194/acp-19-11303-2019, 2019.

Wang, D., Shen, Z., Yang, X., Huang, S., Luo, Y., Bai, G., and Cao, J.: Insight into the Role of NH_3/NH_4^+ and NO_x/NO_3^- in the Formation of Nitrogen-Containing Brown Carbon in Chinese Megacities, Environ. Sci. Technol., 58, 4281-4290, 10.1021/acs.est.3c10374, 2024.

Wang, J., Sun, S., Zhang, C., Xue, C., Liu, P., Zhang, C., Mu, Y., Wu, H., Wang, D., Chen, H., and Chen, J.: The pollution levels, variation characteristics, sources and implications of atmospheric carbonyls in a typical rural area of North China Plain during winter, Journal of Environmental Sciences, 95, 256-265,

https://doi.org/10.1016/j.jes.2020.05.003, 2020.

Wang, J., Ye, J., Zhang, Q., Zhao, J., Wu, Y., Li, J., Liu, D., Li, W., Zhang, Y., Wu, C., Xie, C., Qin, Y., Lei, Y., Huang, X., Guo, J., Liu, P., Fu, P., Li, Y., Lee, H. C., Choi, H., Zhang, J., Liao, H., Chen, M., Sun, Y., Ge, X., Martin, S. T., and Jacob, D. J.: Aqueous production of secondary organic aerosol from fossil-fuel emissions in winter Beijing haze, P. Natl. Acad. Sci. USA, 118, e2022179118, doi:10.1073/pnas.2022179118, 2021a.

Wang, K., Zhang, Y., Huang, R.-J., Cao, J., and Hoffmann, T.: UHPLC-Orbitrap mass spectrometric characterization of organic aerosol from a central European city (Mainz, Germany) and a Chinese megacity (Beijing), Atmos. Environ., 189, 22-29, https://doi.org/10.1016/j.atmosenv.2018.06.036, 2018.

Wang, K., Huang, R.-J., Brueggemand, M., Zhang, Y., Yang, L., Ni, H., Guo, J., Wang, M., Han, J., Bilde, M., Glasius, M., and Hoffmann, T.: Urban organic aerosol composition in eastern China differs from north to south: molecular insight from a liquid chromatography-mass spectrometry (Orbitrap) study, Atmos. Chem. Phys., 21, 9089-9104, https://doi.org/10.5194/acp-21-9089-2021, 2021b.

Wang, Y., Zhao, Y., Li, Z., Li, C., Yan, N., and Xiao, H.: Importance of Hydroxyl Radical Chemistry in Isoprene Suppression of Particle Formation from α-Pinene Ozonolysis, ACS Earth Space Chem., 5, 487-499, https://doi.org/10.1021/acsearthspacechem.0c00294, 2021c.

Wang, Y., Zhuang, G., Zhang, X., Huang, K., Xu, C., Tang, A., Chen, J., and An, Z.: The ion chemistry, seasonal cycle, and sources of $PM_{2.5}$ and TSP aerosol in Shanghai, Atmos. Environ., 40, 2935-2952, https://doi.org/10.1016/j.atmosenv.2005.12.051, 2006.

Wang, Y., Hu, M., Lin, P., Guo, Q., Wu, Z., Li, M., Zeng, L., Song, Y., Zeng, L., Wu, Y., Guo, S., Huang, X., and He, L.: Molecular Characterization of Nitrogen-Containing Organic Compounds in Humic-like Substances Emitted from Straw Residue Burning, Environ. Sci. Technol., 51, 5951-5961, https://doi.org/10.1021/acs.est.7b00248, 2017.

Wang, Y., Hu, M., Hu, W., Zheng, J., Niu, H., Fang, X., Xu, N., Wu, Z., Guo, S., Wu, Y., Chen, W., Lu, S., Shao, M., Xie, S., Luo, B., and Zhang, Y.: Secondary Formation of Aerosols Under Typical High-Humidity Conditions in Wintertime Sichuan Basin, China: A Contrast to the North China Plain, J. Geophys. Res.-Atmos., 126, e2021JD034560, https://doi.org/10.1029/2021JD034560, 2021d.

Wen, W., Shi, L., Li, L., Wang, L., and Chen, J.: Molecular characteristics of ambient organic aerosols in Shanghai winter before and after the COVID-19 outbreak, Sci. Total Environ., 869, 161811, https://doi.org/10.1016/j.scitotenv.2023.161811, 2023.

Wu, Z., Wang, Y., Tan, T., Zhu, Y., Li, M., Shang, D., Wang, H., Lu, K., Guo, S., Zeng, L., and Zhang, Y.: Aerosol Liquid Water Driven by Anthropogenic Inorganic

Salts: Implying Its Key Role in Haze Formation over the North China Plain, Environ. Sci. Technol. Lett., 5, 160-166, 10.1021/acs.estlett.8b00021, 2018.

Xi, Y., Wang, Q., Zhu, J., Yang, M., Hao, T., Chen, Y., Zhang, Q., He, N., and Yu, G.: Atmospheric wet organic nitrogen deposition in China: Insights from the national observation network, Sci. Total Environ., 898, 165629, https://doi.org/10.1016/j.scitotenv.2023.165629, 2023.

Xiao, H.-Y. and Liu, C.-Q.: Chemical characteristics of water-soluble components in TSP over Guiyang, SW China, 2003, Atmos. Environ., 38, 6297-6306, https://doi.org/10.1016/j.atmosenv.2004.08.033, 2004.

Xu, B., Zhang, G., Gustafsson, Ö., Kawamura, K., Li, J., Andersson, A., Bikkina, S., Kunwar, B., Pokhrel, A., Zhong, G., Zhao, S., Li, J., Huang, C., Cheng, Z., Zhu, S., Peng, P., and Sheng, G.: Large contribution of fossil-derived components to aqueous secondary organic aerosols in China, Nature Communications, 13, 5115, 10.1038/s41467-022-32863-3, 2022a.

Xu, Y., Xiao, H., Wu, D., and Long, C.: Abiotic and Biological Degradation of Atmospheric Proteinaceous Matter Can Contribute Significantly to Dissolved Amino Acids in Wet Deposition, Environ. Sci. Technol., 54, 6551-6561, 10.1021/acs.est.0c00421, 2020a.

Xu, Y., Dong, X.-N., Xiao, H.-Y., He, C., and Wu, D.-S.: Water-Insoluble Components in Rainwater in Suburban Guiyang, Southwestern China: A Potential

Contributor to Dissolved Organic Carbon, J. Geophys. Res.-Atmos., 127, e2022JD037721, https://doi.org/10.1029/2022JD037721, 2022b.

Xu, Y., Dong, X.-N., Xiao, H.-Y., Zhou, J.-X., and Wu, D.-S.: Proteinaceous Matter and Liquid Water in Fine Aerosols in Nanchang, Eastern China: Seasonal Variations, Sources, and Potential Connections, J. Geophys. Res.-Atmos., 127, e2022JD036589, https://doi.org/10.1029/2022JD036589, 2022c.

Xu, Y., Dong, X. N., He, C., Wu, D. S., Xiao, H. W., and Xiao, H. Y.: Mist cannon trucks can exacerbate the formation of water-soluble organic aerosol and $PM_{2.5}$ pollution in the road environment, Atmos. Chem. Phys., 23, 6775-6788, https://doi.org/10.5194/acp-23-6775-2023, 2023.

Xu, Y., Lin, X., Sun, Q.-B., Xiao, H.-W., Xiao, H., and Xiao, H.-Y.: Elaborating the Atmospheric Transformation of Combined and Free Amino Acids From the Perspective of Observational Studies, J. Geophys. Res.-Atmos., 129, e2024JD040730, https://doi.org/10.1029/2024JD040730, 2024a.

Xu, Y., Liu, T., Ma, Y. J., Sun, Q. B., Xiao, H. W., Xiao, H., Xiao, H. Y., and Liu, C. Q.: Measurement report: Occurrence of aminiums in PM2.5 during winter in China – aminium outbreak during polluted episodes and potential constraints, Atmos. Chem. Phys., 24, 10531-10542, 10.5194/acp-24-10531-2024, 2024b.

Xu, Y., Miyazaki, Y., Tachibana, E., Sato, K., Ramasamy, S., Mochizuki, T., Sadanaga, Y., Nakashima, Y., Sakamoto, Y., Matsuda, K., and Kajii, Y.: Aerosol

Liquid Water Promotes the Formation of Water-Soluble Organic Nitrogen in Submicrometer Aerosols in a Suburban Forest, Environ. Sci. Technol., 54, 1406-1414, https://dx.doi.org/10.1021/acs.est.9b05849, 2020b.

Yan, F., Su, H., Cheng, Y., Huang, R., Liao, H., Yang, T., Zhu, Y., Zhang, S., Sheng, L., Kou, W., Zeng, X., Xiang, S., Yao, X., Gao, H., and Gao, Y.: Frequent haze events associated with transport and stagnation over the corridor between the North China Plain and Yangtze River Delta, Atmos. Chem. Phys., 24, 2365-2376, 10.5194/acp-24-2365-2024, 2024.

Yang, L., Huang, R.-J., Yuan, W., Huang, D. D., and Huang, C.: pH-Dependent Aqueous-Phase Brown Carbon Formation: Rate Constants and Implications for Solar Absorption and Atmospheric Photochemistry, Environ. Sci. Technol., 58, 1236-1243, 10.1021/acs.est.3c07631, 2024a.

Yang, T., Xu, Y., Ma, Y.-J., Wang, Y.-C., Yu, J. Z., Sun, Q.-B., Xiao, H.-W., Xiao, H.-Y., and Liu, C.-Q.: Field Evidence for Constraints of Nearly Dry and Weakly Acidic Aerosol Conditions on the Formation of Organosulfates, Environ. Sci. Technol. Lett., 11, 981-987, 10.1021/acs.estlett.4c00522, 2024b.

Yang, T., Xu, Y., Ye, Q., Ma, Y. J., Wang, Y. C., Yu, J. Z., Duan, Y. S., Li, C. X., Xiao, H. W., Li, Z. Y., Zhao, Y., and Xiao, H. Y.: Spatial and diurnal variations of aerosol organosulfates in summertime Shanghai, China: potential influence of photochemical processes and anthropogenic sulfate pollution, Atmos. Chem. Phys., 23,

13433-13450, https://doi.org/10.5194/acp-23-13433-2023, 2023.

Yang, X., Huang, S., Li, D., Xu, H., Zeng, Y., Yang, L., Wang, D., Zhang, N., Cao, J., and Shen, Z.: Water-soluble organic matter with various polarities in PM2.5 over Xi'an, China: Abundance, functional groups, and light absorption, Particuology, 84, 281-289, https://doi.org/10.1016/j.partic.2023.07.005, 2024c.

Yassine, M. M., Harir, M., Dabek-Zlotorzynska, E., and Schmitt-Kopplin, P.: Structural characterization of organic aerosol using Fourier transform ion cyclotron resonance mass spectrometry: Aromaticity equivalent approach, Rapid Commun. Mass Spectrom., 28, 2445-2454, https://doi.org/10.1002/rcm.7038, 2014.

Yu, X., Pan, Y., Song, W., Li, S., Li, D., Zhu, M., Zhou, H., Zhang, Y., Li, D., Yu, J., Wang, X., and Wang, X.: Wet and Dry Nitrogen Depositions in the Pearl River Delta, South China: Observations at Three Typical Sites With an Emphasis on Water-Soluble Organic Nitrogen, J. Geophys. Res.-Atmos., 125, e2019JD030983, https://doi.org/10.1029/2019JD030983, 2020.

Yuan, W., Huang, R.-J., Shen, J., Wang, K., Yang, L., Wang, T., Gong, Y., Cao, W., Guo, J., Ni, H., Duan, J., and Hoffmann, T.: More water-soluble brown carbon after the residential “coal-to-gas” conversion measure in urban Beijing, npj Climate and Atmospheric Science, 6, 20, 10.1038/s41612-023-00355-w, 2023.

Zeng, Y., Ning, Y., Shen, Z., Zhang, L., Zhang, T., Lei, Y., Zhang, Q., Li, G., Xu, H., Ho, S. S. H., and Cao, J.: The Roles of N, S, and O in Molecular Absorption

Features of Brown Carbon in $PM_{2.5}$ in a Typical Semi-Arid Megacity in Northwestern China, J. Geophys. Res.-Atmos., 126, e2021JD034791, https://doi.org/10.1029/2021JD034791, 2021.

Zhang, B., Shen, Z., He, K., Zhang, L., Huang, S., Sun, J., Xu, H., Li, J., Yang, L., and Cao, J.: Source Profiles of Particle-Bound Phenolic Compounds and Aromatic Acids From Fresh and Aged Solid Fuel Combustion: Implication for the Aging Mechanism and Newly Proposed Source Tracers, J. Geophys. Res.-Atmos., 128, e2023JD039758, https://doi.org/10.1029/2023JD039758, 2023a.

Zhang, H., He, P., Liu, L., Dai, H., Zhao, B., Zeng, Y., Bi, J., Liu, M., and Ji, J. S.: Trade-offs between cold protection and air pollution–induced mortality of China's heating policy, PNAS Nexus, 2, 10.1093/pnasnexus/pgad387, 2023b.

Zhang, T., Cao, J. J., Tie, X. X., Shen, Z. X., Liu, S. X., Ding, H., Han, Y. M., Wang, G. H., Ho, K. F., Qiang, J., and Li, W. T.: Water-soluble ions in atmospheric aerosols measured in Xi'an, China: Seasonal variations and sources, Atmos. Res., 102, 110-119, https://doi.org/10.1016/j.atmosres.2011.06.014, 2011.

Zhang, Y.-L. and Cao, F.: Fine particulate matter ($PM_{2.5}$) in China at a city level, Scientific Reports, 5, 14884, 10.1038/srep14884, 2015.

Zhang, Z., Guan, H., Xiao, H., Liang, Y., Zheng, N., Luo, L., Liu, C., Fang, X., and Xiao, H.: Oxidation and sources of atmospheric NO_x during winter in Beijing based on $\delta^{18}O$-$\delta^{15}N$ space of particulate nitrate, Environmental Pollution, 276, 116708,

https://doi.org/10.1016/j.envpol.2021.116708, 2021a.

Zhang, Z., Zhou, Y., Zhao, N., Li, H., Tohniyaz, B., Mperejekumana, P., Hong, Q., Wu, R., Li, G., Sultan, M., Zayan, A. M. I., Cao, J., Ahmad, R., and Dong, R.: Clean heating during winter season in Northern China: A review, Renewable and Sustainable Energy Reviews, 149, 111339, https://doi.org/10.1016/j.rser.2021.111339, 2021b.

Zhao, D. and Sun, B.: Atmospheric Pollution from Coal Combustion in China, Journal of the Air Pollution Control Association, 36, 371-374, 10.1080/00022470.1986.10466074, 1986.

Zheng, P., Chen, Y., Wang, Z., Liu, Y., Pu, W., Yu, C., Xia, M., Xu, Y., Guo, J., Guo, Y., Tian, L., Qiao, X., Huang, D. D., Yan, C., Nie, W., Worsnop, D. R., Lee, S., and Wang, T.: Molecular Characterization of Oxygenated Organic Molecules and Their Dominating Roles in Particle Growth in Hong Kong, Environ. Sci. Technol., 10.1021/acs.est.2c09252, 2023.